Local and Modal Damage Indicators for Reinforced Concrete Shear Frames Subject to Earthquakes

Köylüoglu, H. U.; Nielsen, Søren R. K.; Abbott, J.; Cakmak, A. S.

Publication date:
1995

Document Version
Publisher's PDF, also known as Version of record

INSTITUTTET FOR BYGNINGSTEKNIK
DEPT. OF BUILDING TECHNOLOGY AND STRUCTURAL ENGINEERING
AALBORG UNIVERSITET • AUC • AALBORG • DANMARK

STRUCTURAL RELIABILITY THEORY
PAPER NO. 145

Submitted to Journal of Engineering Mechanics, ASCE

H. U. KÖYLÜOĞLU, S. R. K. NIELSEN, J. ABBOTT & A. Ş. ÇAKMAK
LOCAL AND MODAL DAMAGE INDICATORS FOR REINFORCED CONCRETE SHEAR FRAMES SUBJECT TO EARTHQUAKES
AUGUST 1995 ISSN 0902-7513 R9521

The STRUCTURAL RELIABILITY THEORY papers are issued for early dissemination of research results from the Structural Reliability Group at the Department of Building Technology and Structural Engineering, University of Aalborg. These papers are generally submitted to scientific meetings, conferences or journals and should therefore not be widely distributed. Whenever possible reference should be given to the final publications (proceedings, journals, etc.) and not to the Structural Reliability Theory papers.

Printed at Aalborg University

INSTITUTTET FOR BYGNINGSTEKNIK
DEPT. OF BUILDING TECHNOLOGY AND STRUCTURAL ENGINEERING
AALBORG UNIVERSITET • AUC • AALBORG • DANMARK

STRUCTURAL RELIABILITY THEORY
PAPER NO. 145

Submitted to Journal of Engineering Mechanics, ASCE

H. U. KÖYLÜOĞLU, S. R. K. NIELSEN, J. ABBOTT & A. Ş. ÇAKMAK
LOCAL AND MODAL DAMAGE INDICATORS FOR REINFORCED CONCRETE SHEAR FRAMES SUBJECT TO EARTHQUAKES
AUGUST 1995 ISSN 0902-7513 R9521

LOCAL AND MODAL DAMAGE INDICATORS FOR REINFORCED CONCRETE SHEAR FRAMES SUBJECT TO EARTHQUAKES

H. Uğur Köylüoğlu
College of Arts and Sciences
Koç University, 80860 İstinye, İstanbul, Turkey

Søren R. K. Nielsen
Dept. of Structural Engineering and Building Technology
Aalborg University, DK-9000 Aalborg, Denmark

Jamison Abbott
Dept. of Civil Engineering and Operations Research
Princeton University, Princeton, NJ 08544, USA

Ahmet Ş. Çakmak
Dept. of Civil Engineering and Operations Research
Princeton University, Princeton, NJ 08544, USA

ABSTRACT

Local, modal and overall damage indicators for reinforced concrete shear frames subject to seismic excitation are defined and studied. Each storey of the shear frame is represented by a Clough and Johnston hysteretic oscillator with degrading elastic fraction of the restoring force. The local maximum softening damage indicators are defined in a closed form based on the variation of the eigenfrequency of the local oscillators due to the local stiffness and strength deterioration. The modal maximum softening damage indicators are calculated from the variation of the eigenfrequencies of the structure during the excitation. The linear and nonlinear parameters of the local oscillators are assumed to be known. Next, a statistical analysis is performed where a sample 5 storey shear frame is subject to sinusoidal and simulated earthquake excitations. The shear frame is subject to 30 independent simulations of the earthquake excitation which is modeled as a stationary Gaussian stochastic process with Kanai-Tajimi Spectrum, multiplied by an envelope function. Equations of motion of the storeys are solved by a Runge-Kutta fourth order scheme where the local softening value is recorded. The modal maximum softening indicators are calculated from the known instantaneous stiffness matrix which is a function of structural properties and local damage. Alternatively, a Fourier analysis is performed for consecutive time-windows to measure the same evolution using the top storey displacement. Finally, the relationship between local and modal damage indices are investigated statistically.

1. INTRODUCTION

The purpose of this study is to derive a non-linear mechanical formulation to quantify local, modal and overall damage in reinforced concrete (RC) multi-degree-of-freedom

(MDOF) shear frames subject to earthquakes.

The physical local damage in RC structures subject to severe seismic excitation is attributed to micro-cracking and crushing of concrete, yielding of the reinforcement bars and bond deterioration at the steel-concrete interfaces. To the extent that RC structures can be modelled by non-linear mechanical theories, local damage at a cross-section of the structure can adequately be measured by the degradation of bending stiffness and moment capacity of the cross-section. In a shear frame, this is numerically tantamount to a reduction in the column stiffnesses. Overall effect of all local damages is the stiffness and strength deterioration of the structure. A global damage indicator can then be defined as a functional of such continuously distributed local damages which characterize the overall damage state and serviceability of the structure.

Local and global damage indicators are response quantities characterizing the damage state of the structure after an earthquake excitation, and such can be used in decision-making during the design phase, or in case of post-earthquake reliability and repair problems. In serving these purposes, the damage indicators should, at least, be observable for practical purposes, be a non-decreasing function of time unless the structure is repaired or strengthened, possess a failure surface (serviceability or ultimate limit state) to separate safe states from the unsafe ones and carry Markov property so that post-earthquake reliability estimates for a partly damaged element or structure can be estimated solely from the latest recorded value of the damage indicator.

The maximum softening damage indicators (MSDI) measure the maximum relative reduction of the vibrational frequencies for an equivalent linear system with slowly varying stiffness properties during a seismic event, hence, display the combined damaging effects of the maximum displacement ductility of the structure during extreme plastic deformations and the stiffness deterioration in the elastic regime, the latter effect being referred as final softening. The introduction of the one-dimensional modal MSDI based on an equivalent linear single-degree-of-freedom (SDOF) system fit to the first mode of the RC building as a global damage indicator is due to DiPasquale and Çakmak (1990). The excitation and displacement response time series of a single position on the building are the only required observations for the one-dimensional modal MSDI. The applicability of the index was analysed based on data from shake table experiments with RC frames performed by Sözen and his associates (Çeçen 1978, Healey and Sözen 1979). Limit states for slight damage to total collapse were calibrated using this data and the performance of the index was tested for partly damaged structures which had been instrumented in the past. The modal MSDI concept has also been generalized to MDOF models along with the associated damage localization problem Nielsen et al. (1993). The Markov property of the modal MSDI chains for SDOF and 2DOF models was tested numerically by means of Monte Carlo simulations, Nielsen et al. (1992, 1993), and it was concluded that the modal damage indicators fulfill Markov property with sufficient accuracy. The prediction of global and localized damage and the future reliability estimation of partly damaged RC structures under seismic excitation were studied recently, Köylüoğlu et al. (1994). A hysteretic model is suited to the first mode such that the first mode is modelled as a Clough and Johnston hysteretic oscillator, (Clough and Johnston, 1966), with degrading elastic fraction of the restoring force, su-

bject to seismic excitation. The linear system parameters are assumed to be known, measured before the arrival of the first earthquake from nondestructive vibration tests or via structural analysis. Previous excitation and displacement response time series is employed for the identification of the instantaneous softening using an ARMA model. The two free hysteresis parameters are updated after each earthquake from a system identification procedure where a weighted error criteria defined on instantaneous softening and the displacement response time series is employed. The performance of the model is illustrated on RC frames which were tested by Sözen and his associates.

Damage indicators based on the changes in the natural frequencies of structures have also been used by other researchers, e.g. Hassiotis and Jeong (1993), Jajela and Soeiro (1990). Both studies are performed to determine the local damage based on information about the changes in the eigenfrequencies of the structure. Hassiotis and Jeong (1993) proposed a quadratic optimization formulation to solve the arising undetermined equations with a suitable optimization criterion. They concluded that reduction in stiffness up to 40 percent at single and multiple sites can be detected when perfectly measured data is used. It is also noted that when the data used is polluted randomly, light damage cannot be detected.

Rahman and Grigoriu (1994) related the hysteretic behaviour of the storey columns to the storey level degree of freedom analytically. They derived these relationships using hysteretic constitutive laws and quantified damage using an energy-based rule. Based on numerical studies, it is concluded that the global model, the storey level one, provides good estimates of seismic response quantities compared to the local model, the storey columns.

In this paper, the hysteretic model proposed in Köylüoğlu et al. (1994) is generalized for MDOF systems to calculate local damage by representing each storey of the shear frame as a Clough and Johnston hysteretic oscillator. The local MSDI is then defined in a closed form based on the variation of the eigenfrequency of the local oscillators due to the local stiffness and strength deterioration. In what follows, the MDOF hysteretic model for RC shear frames is derived and numerical analysis is carried out for a sample 5 storey shear frame subject to sinusoidal and earthquake excitations with the same energy content and different frequencies matching the first three modes. The linear and nonlinear parameters of the local oscillators are assumed to be known. The linear parameters can be calculated from structural analysis or nondestructive testing. The nonlinear parameters can be obtained from experimentation and/or analytic derivations as given in Rahman and Grigoriu (1994). This uses the fact that all storey level mass is lumped at the storey level and a single degree of freedom is assigned for the storey displacement which is the displacement of the tip of the columns carrying the storey. The shear frame is subject to sinusoidal input and simulations of the earthquake excitation which is modeled as a stationary Gaussian stochastic process with Kanai-Tajimi Spectrum, multiplied by an envelope function. Equations of motion of the storeys are solved using a Runge-Kutta fourth order scheme where the local softening value is recorded. The modal maximum softening indicators are calculated from the known instantaneous stiffness matrix which is a function of structural properties and local damage. Instantaneous global stiffness matrix is known for design purposes and changes locally when a

yielding occurs. For post-earthquake analyis, alternatively, performing a Fourier analysis for consecutive time-windows to measure the evolution of modal softening using the ground excitation and the top storey displacement time series relative to the ground surface is suggested, Mullen et al. (1995). Finally, the relationship between local, modal and overall damage indices are investigated statistically.

2. HYSTERETIC MODEL FOR MDOF SHEAR FRAMES

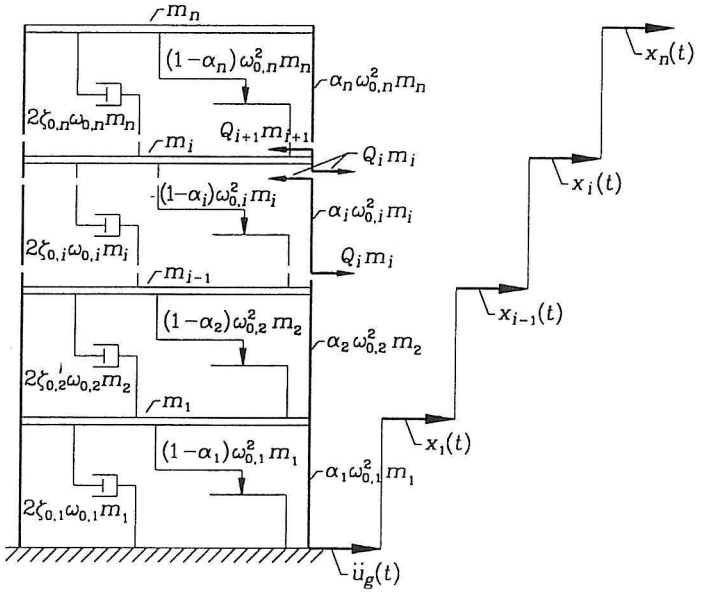

Figure 1. MDOF shear frame with local hysteretic oscillators.

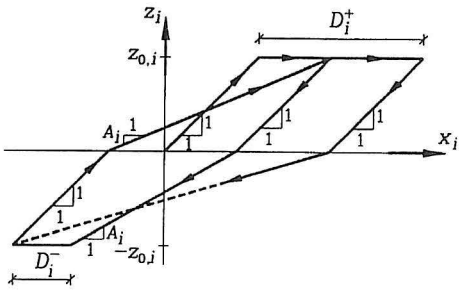

Figure 2. Clough-Johnston hysteretic model.

Consider an n storey RC shear frame. The relative displacement between the ith and $(i+1)$th storeys is designated as x_i and x_1 signifies the displacement of the first storey relative to ground surface excited by the horizontal acceleration $\ddot{u}_g$, see Figure 1. For simplicity, the time dependence of $x, \ddot{u}_g$ etc. is not explicitly shown in the following notation. With reference to the shear model shown in Figure 1, the relative displacement x_i between the ith and $(i+1)$th storey is assumed to cause a shear force of magnitude $Q_i m_i$ where m_i is the storey mass. The equations of motion in terms of the relative displacements can be written as

$$\left.\begin{aligned}
\ddot{x}_1 &= \mu_2 Q_2 - Q_1 - \ddot{u}_g && , \quad t > 0 \\
\ddot{x}_i &= \mu_{i+1} Q_{i+1} - (\mu_i + 1) Q_i + Q_{i-1}, && t > 0 \qquad , \quad i = 2, 3, \cdots, n-1 \\
\ddot{x}_n &= -(\mu_n + 1) Q_n + Q_{n-1} && , \quad t > 0 \\
x_i(0) &= \dot{x}_i(0) = 0 && , \quad i = 1, 2, \cdots, n
\end{aligned}\right\} \qquad (1)$$

$$\mu_i = \frac{m_i}{m_{i-1}} \quad , \quad i = 2, 3, \cdots, n \tag{2}$$

$$Q_i = 2\zeta_{0,i}\omega_{0,i}\dot{x}_i + \omega_{0,i}^2\big(\alpha_i x_i + (1-\alpha_i)z_i\big) \quad , \quad i = 1, 2, \cdots, n \tag{3}$$

$$\dot{z}_i = k(\dot{x}_i, z_i, D_i; z_{0,i})\dot{x}_i \quad , \quad t > 0 \quad , \quad z_i(0) = 0 \quad , \quad i = 1, 2, \cdots, n \tag{4}$$

$$\dot{D}_i = g(\dot{x}_i, z_i; z_{0,i})\dot{x}_i \quad , \quad t > 0 \quad , \quad D_i(0) = D_{0,i} \quad , \quad i = 1, 2, \cdots, n \tag{5}$$

$$\alpha_i = \Big(\frac{2z_{0,i}}{2z_{0,i} + D_i}\Big)^{n_{0,i}} \quad , \quad i = 1, 2, \cdots, n \tag{6}$$

$$k\big(\dot{x}_i, z_i, D_i; z_{0,i}\big) = H(z_i)\big\{A_i H(\dot{x}_i)(1 - H(z_i - z_{0,i})) + H(-\dot{x}_i)\big\} +$$

$$H(-z_i)\big\{A_i H(-\dot{x}_i)(1 - H(-z_i - z_{0,i})) + H(\dot{x}_i)\big\} \quad , \quad i = 1, 2, \cdots, n \tag{7}$$

$$g\big(\dot{x}_i, z_i; z_{0,i}\big) = H(\dot{x}_i)H(z_i - z_{0,i}) - H(-\dot{x}_i)H(-z_i - z_{0,i}) \quad , \quad i = 1, 2, \cdots, n \tag{8}$$

$$A_i = \frac{z_{0,i}}{z_{0,i} + D_i} \quad , \quad i = 1, 2, \cdots, n \tag{9}$$

$$H(x) = \begin{cases} 1 & , \quad x \geq 0 \\ 0 & , \quad x < 0 \end{cases} \tag{10}$$

Equation (1) is derived using Newton's second law of motion. Equation (2) defines μ_i which is the ratio of the lumped mass at the two consecutive storeys. $2\zeta_{0,i}\omega_{0,i}m_i$ and $\omega_{0,i}^2 m_i$ appearing in equation (3) without m_i are respectively the linear viscous damping coefficients and initial elastic spring stiffnesses between the storeys. $\alpha_i\big(D_i\big)$ is the elastic fraction of the restoring force which is a function of damage. z_i is the hysteretic component which is modelled using the Clough-Johnston hysteretic model of Figure 2. $z_i = +z_{0,i}$, $z_i = -z_{0,i}$ signify the yield levels. $k\big(\dot{x}_i, z_i, D_i; z_{0,i}\big)$ is a nonanalytic function describing the state dependent stiffness of the hysteretic model on the component z_i. The stiffness degrading hysteretic constitutive law of the model can be represented as shown in Figure 2. The Clough-Johnston model deals with the stiffness

degradation by changing the slope A_i of the elastic branches as the accumulated plastic deformations D_i^+ and D_i^- at positive and negative yielding, increase as shown in Figure 2. $D_i = D_i^+ + D_i^-$ is the total accumulated plastic deformations. Hence, D_i represents the damage between $(i-1)$th and ith stories in the actual RC structure. For loading branches, the slope A_i is selected such that the elastic branch always aims at the previous unloading point with the other sign. At unloadings, the slope is 1. $D_{0,i}$ is the initial value of the total accumulated damage which is zero before the first earthquake hits and is assumed to be determined from previous earthquake and displacement response records for the succeeding earthquakes. $H(x)$ is the unit step function.

A novelty of the present model stems primarily from the modelling of $\alpha_i(D_i)$ as a non-increasing function of the damage parameter D_i. Since, $\alpha_i(D_i)$ measures the fraction of the restoring force from linear elastic behaviour, this fraction must decrease as larger and larger parts of the structure become plastic. Note that for an undamaged structure, $\alpha_i(D_i(0)) = 1$, and, unless there is damage, still $\alpha_i(0) = 1$. The dependency of $\alpha_i(D_i)$ on D_i as indicated by (6) has been selected to fulfill this boundary condition. The relative success of the model (1)-(10) in reproducing actually recorded displacement time series in the earlier work of the authors is primarily due to this modelling, Köylüoğlu et al. (1994).

The hysteretic parameters $z_{0,i}, n_{0,i}$ should be identified using time-series data of experienced seismic event and system identification or via laboratory testing. The linear parameters can be obtained from a structural analysis or via nondestructive testing.

It should be noted that the Clough-Johnston hysteretic model was originally designed for RC beams. The differential description of the model was first introduced by Minai and Suzuki (1985) for SDOF systems.

3. MODAL MAXIMUM SOFTENING DAMAGE INDICATORS

The instantaneous modal softening for the jth mode, $\delta_j(t)$, of the structure is defined as, Çakmak et al. [3,11,12] :

$$\delta_j(t) = 1 - \frac{T_{0,j}}{T_j(t)} \tag{11}$$

where $T_{0,j}$ is the jth period of the linear structure and $T_j(t)$ is the jth period of the equivalent linear structure with slowly varying stiffness characteristics during an earthquake excitation. $T_{0,j}$ is usually known from previous structural analysis or nondestructive experimentation of the structure and $T_j(t)$ can be either calculated from the instantaneous global stiffness matrix, if available for design purposes, or estimated from the excitation and displacement response time series after an earthquake using a system identification procedure. For example, system identification can be performed in the frequency domain. This requires a Fourier analysis for consecutive time windows to measure the evolution of the eigenfrequencies of the structure.

The jth modal MSDI $\delta_{M,j}$ is defined as the maximum of $\delta_j(t)$ during the seismic excitation.

$$\delta_{M,j} = \max\ \delta_j(t) \quad , \quad j = 1, 2, \cdots, n \tag{12}$$

Hence, jth modal MSDI is a numerical value in between 0 and 1, 0 showing no damage and 1 denoting total loss of stiffness in the corresponding mode, that is the full-collapse.

4. LOCAL MAXIMUM SOFTENING DAMAGE INDICATORS

In the hysteretic model for the ith relative displacement, the instantaneous slope of the hysteretic curve defines the variations of the instantaneous period. For Clough-Johnston model, instantaneous slope is $A_i(t)$ for loading branches, 1 for unloading branches and 0 when yielding occurs. Considering these zeros and ones, instead of instantaneous softening an average softening value is defined using the average slope $\bar{m}_i$ in a hysteresis loop, the slope of the line through extreme points, see Figure 2.

$$\bar{m}_i = \frac{2z_{0,i}}{2z_{0,i} + D_i(t)} \tag{13}$$

The loop-averaged softening $S_i(t)$ is defined as

$$S_i(t) = 1 - \sqrt{\frac{2z_{0,i}}{2z_{0,i} + D_i}(1 - \alpha_i) + \alpha_i} \quad , \quad i = 1, 2, \cdots, n \tag{14}$$

$S_i(t)$ is a local damage indicator displaying the damaging effects of the local plastic deformations. As seen from (14), $S_i(t)$ is non-decreasing during a seismic event and fully correlated to total accumulated plastic deformation $D_i(t)$. It should be noted that both D_i and α_i are time and damage dependent.

The ith local MSDI $S_{M,i}$ is defined as the maximum of $S_i(t)$ which is the final value of $S_i(t)$ during an earthquake.

$$S_{M,i} = \max\ S_i(t) \quad , \quad i = 1, 2, \cdots, n \tag{15}$$

The local damage indicator, $S_i(t)$, takes on numerical values between 0 and 1, 0 denoting no local damage and 1 meaning total collapse of columns under the ith storey. Moreover, the local stiffness reduction percentage is functionally related to $S_i(t)$ as $\left(1 - S_i(t)\right)^2$, e.g. $S_i(t) = 0.4$ means that the local stiffness has been reduced to 36 percent of the initial local stiffness at the ith storey.

5. OVERALL MAXIMUM SOFTENING DAMAGE INDICATORS

A scalar numerical overall damage indicator can be defined as a function of modal or local damages. Overall damage indicators are basically averages of the local or

modal MSDI and are defined to serve for preliminary damage analysis after earthquake excitations. It should be noted that the overall MSDI does not uniquely represent the damage distribution of the structure.

Two scalar numerical overall MSDI are proposed. The first one, overall MSDI based on modal MSDI $\hat{\delta}_M$ is defined as the weighted average of modal MSDI with weights defined as the absolute value of the modal participation factors β_j, $j = 1, 2, \cdots, n$. The weights are chosen as $|\beta_j|$ based on the fact that the modal participation factors denote the contribution of the modes in the overall response in the linear case.

$$\hat{\delta}_M = \frac{\sum_{j=1}^{n} |\beta_j| \delta_{M,j}}{\sum_{j=1}^{n} |\beta_j|} \tag{16}$$

$\hat{\delta}_M$ is called the overall MSDI of the first type. Although the maximum of δ_j do not take place at the same instant for all the modes during the seismic excitation, for simplicity $\hat{\delta}_M$ follows the definition given above.

Another overall MSDI $\hat{S}_M$ is defined as the numerical average of the local MSDI $S_{M,i}$.

$$\hat{S}_M = \frac{1}{n} \sum_{i=1}^{n} S_{M,i} \tag{17}$$

$\hat{S}_M$ is called the overall MSDI of the second type in this paper.

6. THE EVOLUTION OF EIGENFREQUENCIES

The evolution of the eigenfrequencies during a seismic event is needed to calculate the modal MSDI. These can be computed if the instantaneous stiffness matrix is known. For design purposes, since the local damage can be computed from the model at any time instant, the instantaneous local softening can also be estimated and the global stiffness matrix can then be constructed. The local stiffness degradation is related to the local MSDI as

$$k_i(t) = k_{0,i}(1 - S_i(t))^2 \tag{18}$$

where $k_i(t)$ is the instantaneous stiffness of the ith storey. Using such instantaneous local stiffnesses, the instantaneous global stiffness matrix $\mathbf{K}(t)$ can be assembled and an eigenanalysis can be performed to calculate modal MSDI $\delta_{M,j}$.

Alternatively, for post-earthquake damage evaluations, a Fourier analysis can be performed using the base acceleration and top storey displacement time series. This further requires moving time-windows since the evolution of the eigenfrequencies are searched.

In the Fourier analysis, the freqency response function is evaluated and eigenfrequencies are determined approximately from the peaks of this function.

7. NUMERICAL INVESTIGATIONS

A five storey RC shear frame is used to demonstrate the abilities of the hysteretic MDOF model to detect and quantify local, modal and overall damage in shear frames subject to severe excitations.

All storeys are assumed to have the same mass, stiffness and damping characteristics. Thus, $\mu_i = 1$ and the frequencies, damping ratios of the local oscillators are taken as $\omega_{0,i} = 7\pi$ Hertz, $\zeta_{0,i} = 0.03$ for $i = 1, 2, \cdots, n$. The nonlinear parameters are also assumed to be the same for all storeys and taken as $z_{0,i} = 24$ mm and $n_{0,i} = 0.8$ for $i = 1, 2, \cdots, n$. The yield level 24 mm is found to be reasonable by the authors since it correponds to a horizontal strain of 0.008 for a storey of height 3 m.

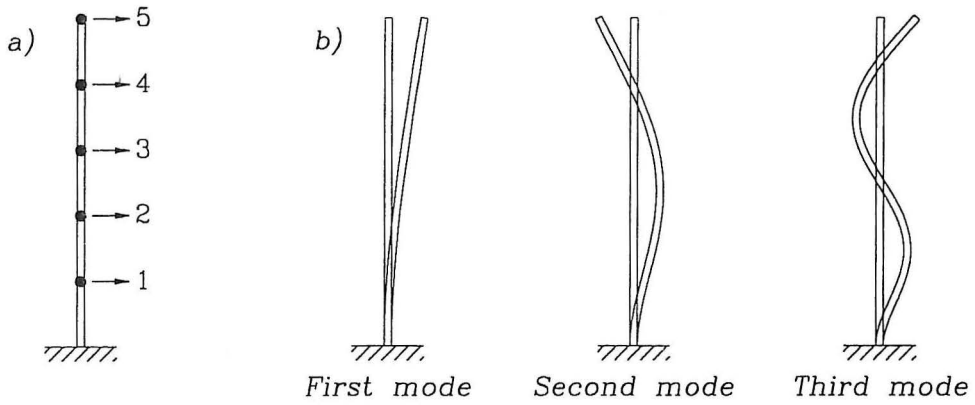

Figure 3. a) 5 DOF model for 5 storey RC shear frame. b) The first three mode shapes.

With these parameters, an eigenvalue analysis is performed, the modal eigenfrequencies and modal damping ratios of the undamaged structure are determined. The mode shapes of the first three modes are given in Figure 3.b, eigenfrequencies, periods and modal damping ratios are listed in Table 1.

Table 1. Eigenfrequencies, periods and modal damping ratios of the 5 storey shear frame

Mode Number	Frequency (Hertz)	Period (sec)	Damping Ratios
1	0.996204	1.003811	0.008539
2	2.907905	0.343890	0.024925
3	4.584025	0.218149	0.039292
4	5.888775	0.169815	0.050475
5	6.716451	0.148888	0.057570

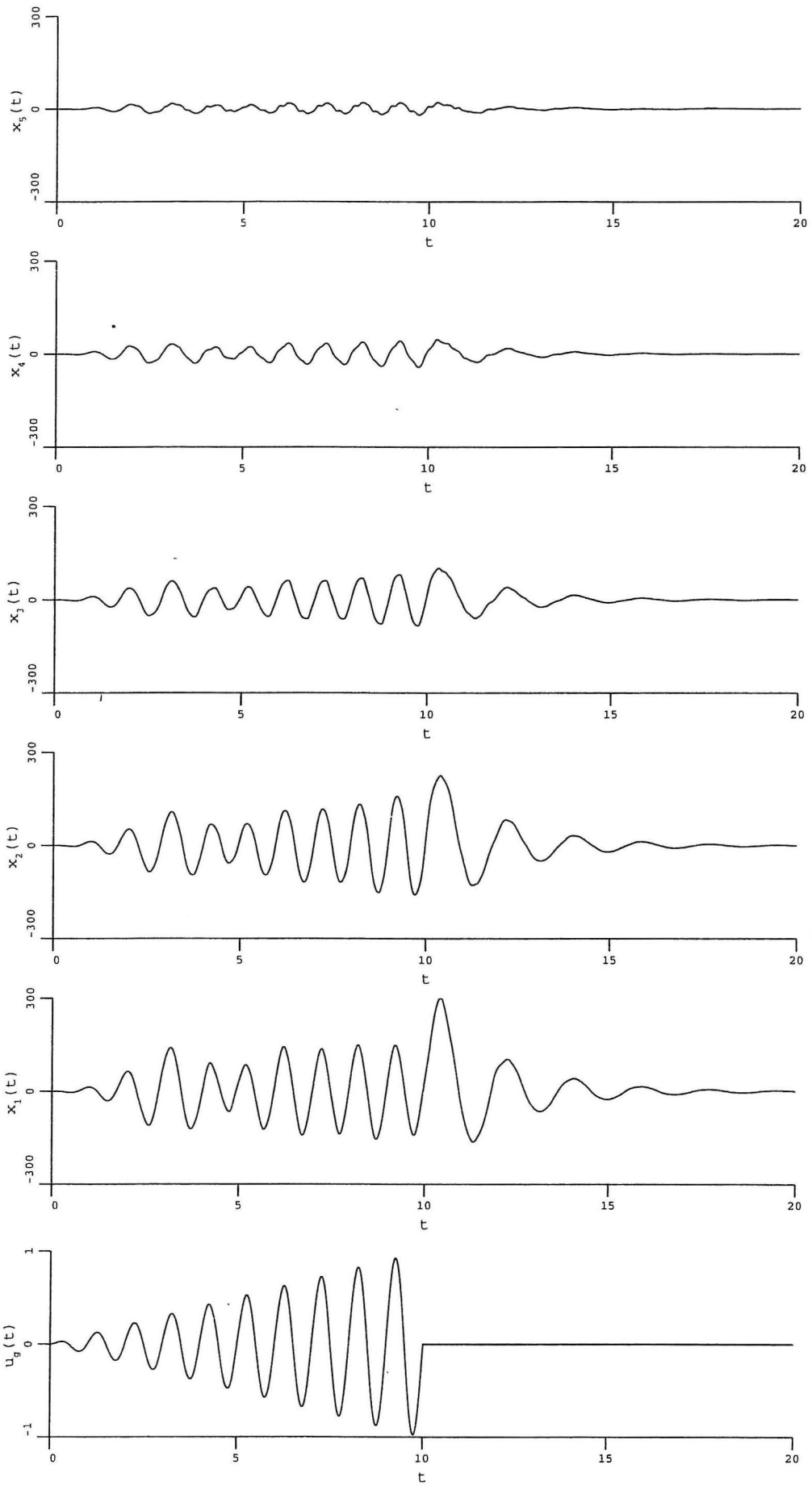

Figure 4. The sine ground acceleration (normalized to g) exciting the first mode and the response of the structure in terms of relative displacements $x_i(t)$ in mm.

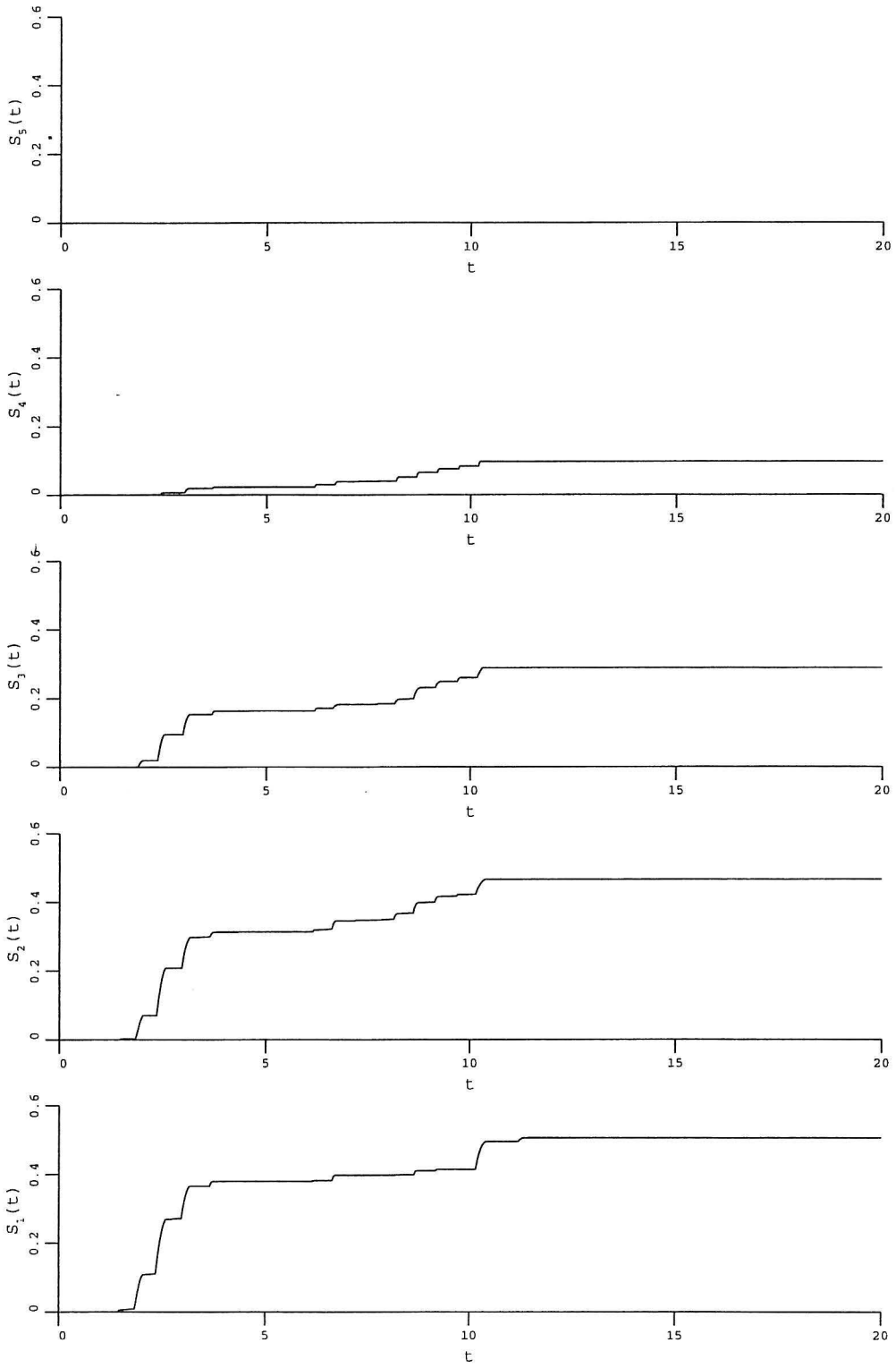

Figure 5. Instantaneous local softening values $S_i(t)$ during the first sine excitation.

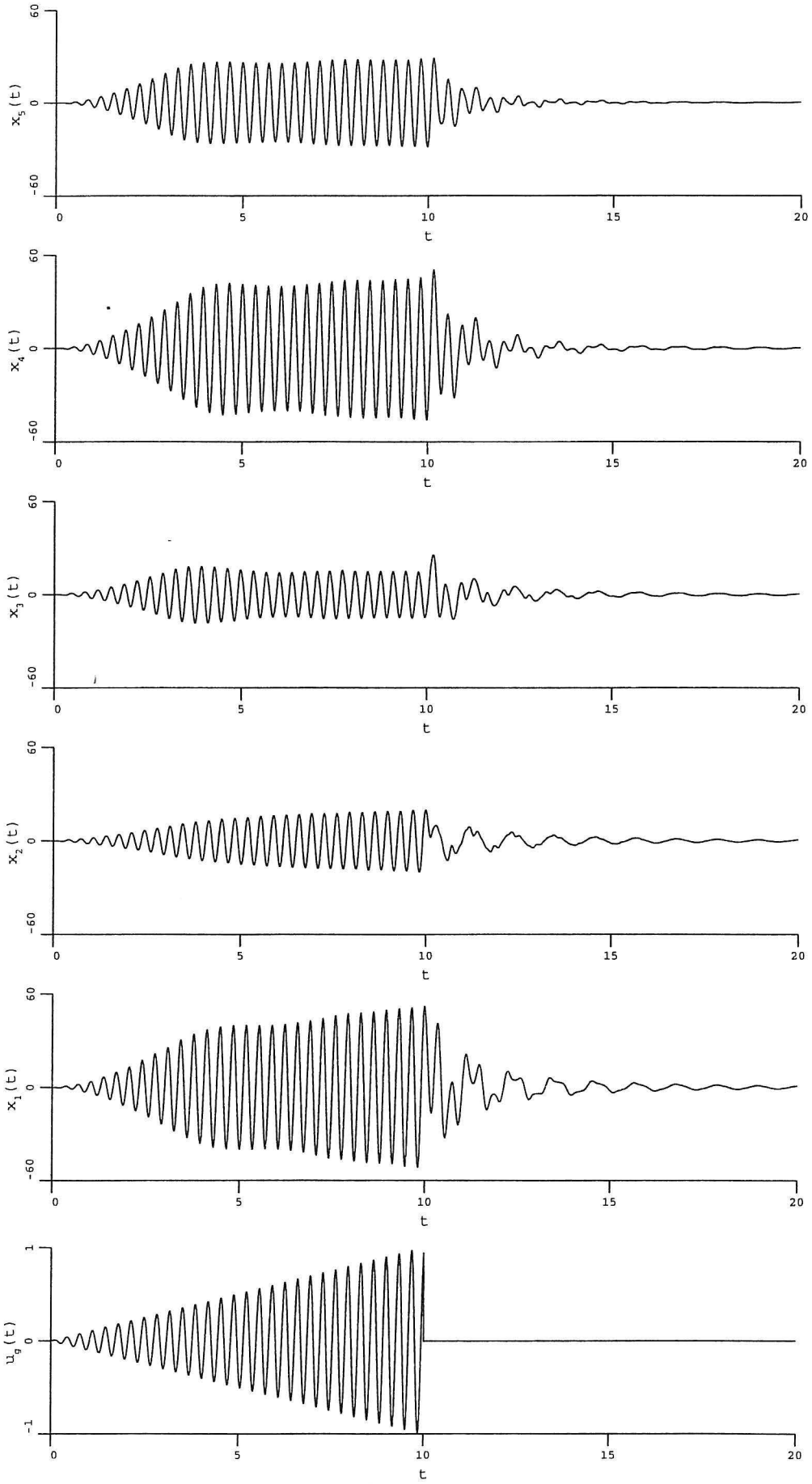

Figure 6. The sine ground acceleration (normalized to g) exciting the second mode and the response of the structure in terms of relative displacements $x_i(t)$ in mm.

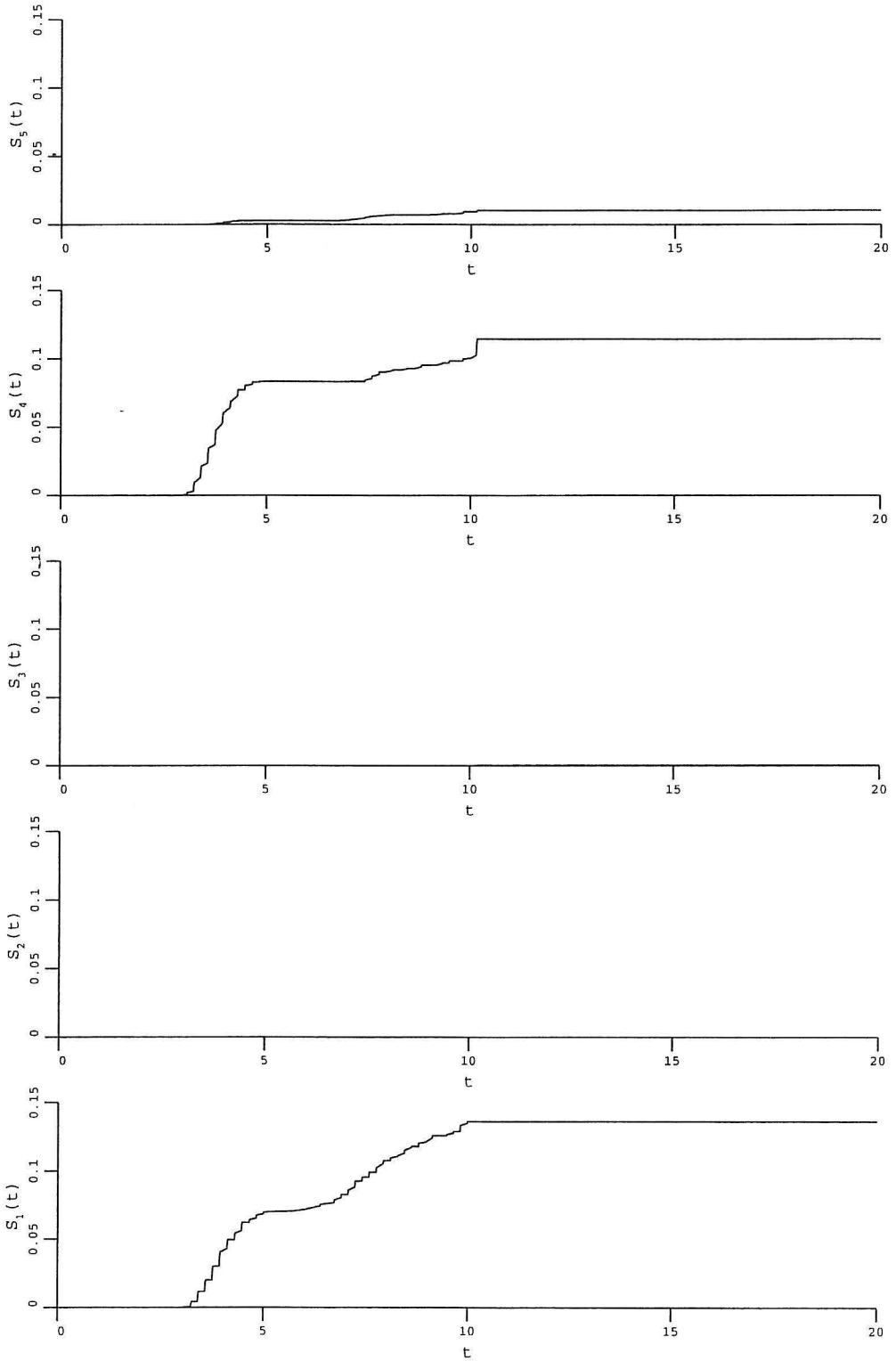

Figure 7. Instantaneous local softening values $S_i(t)$ during the second sine excitation.

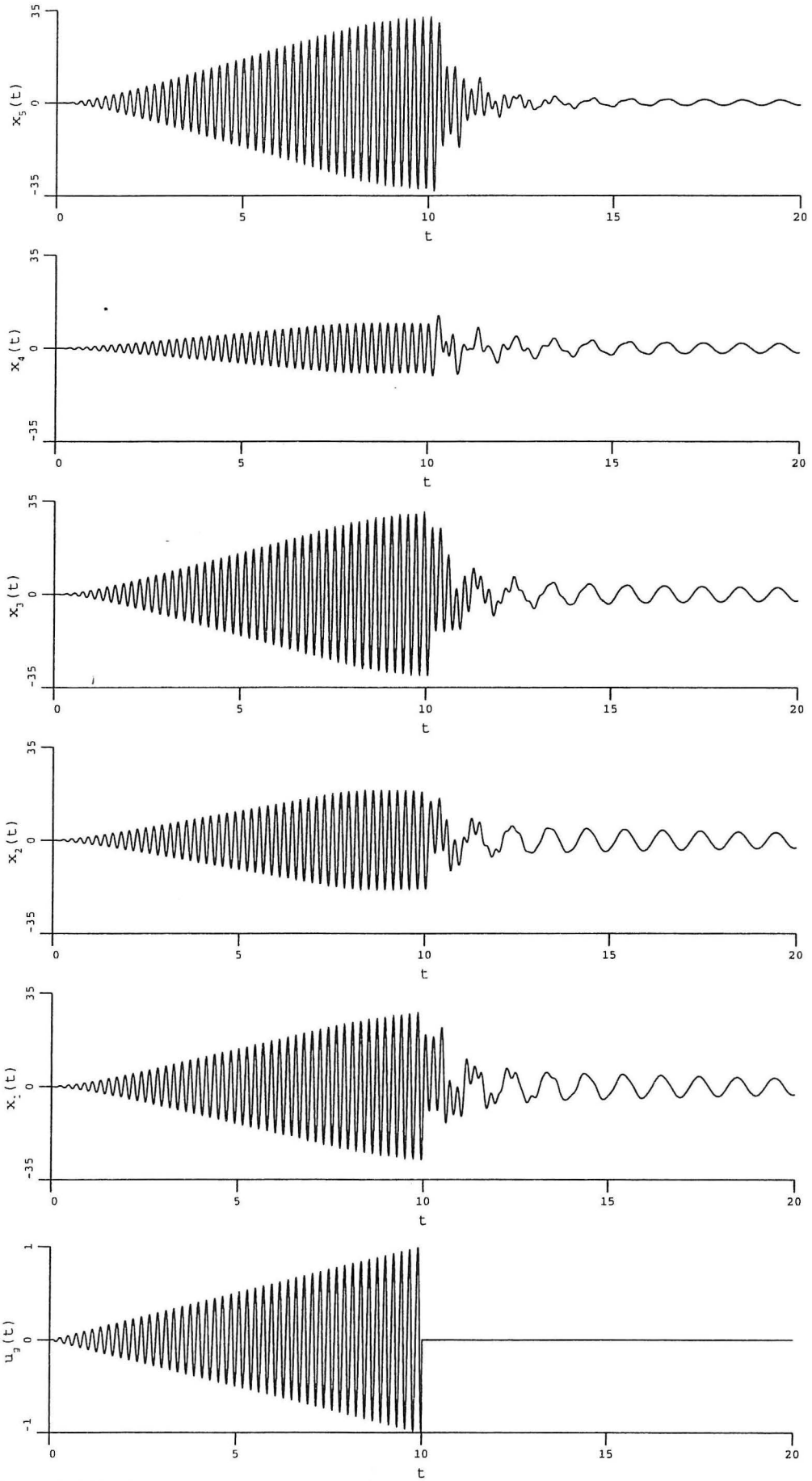

Figure 8. The sine ground acceleration (normalized to g) exciting the third mode and the response of the structure in terms of relative displacements $x_i(t)$ in mm.

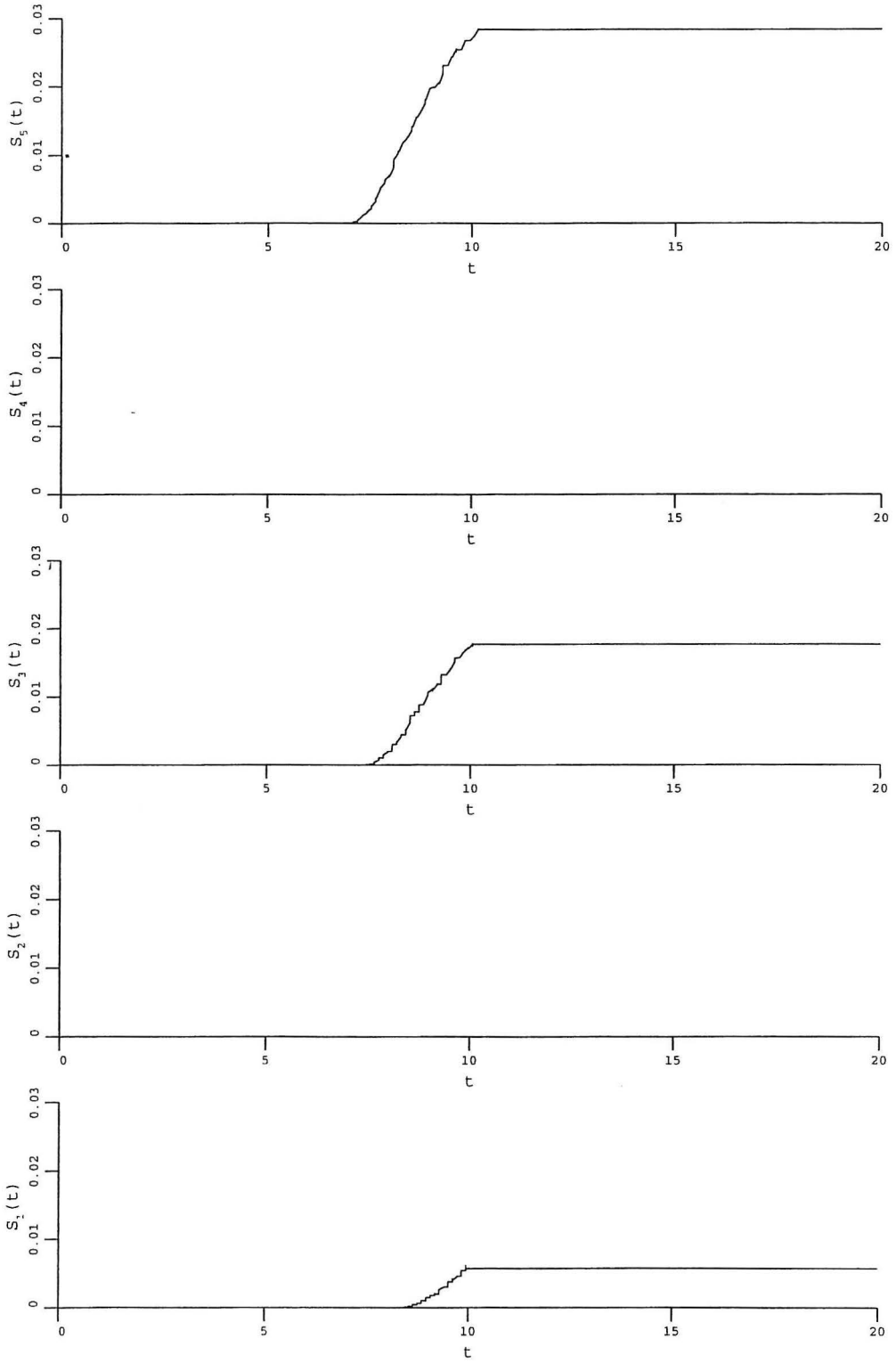

Figure 9. Instantaneous local softening values $S_i(t)$ during the third sine excitation.

The structure is first subject to 3 different sinusoidal loadings as horizontal base accelerations with increasing amplitude and different frequencies, see Figures 4, 6 and 8. These excitations are chosen to excite the first, second and the third mode respectively. The sine excitations reach an amplitude of $1g$ after 10 seconds and the system is let to eigenvibrations after that to observe the eigenvibrations with a large period due to damage and softening in the local oscillators.. Local, modal and overall MSDI of the first and second types are calculated for each input and the results are tabulated in Tables 2 and 3.

Table 2. Sine excitation and the local MSDI and overall MSDI of second type

Excitation	$S_{M,1}$	$S_{M,2}$	$S_{M,3}$	$S_{M,4}$	$S_{M,5}$	$\hat{S}_M$
$0.1\ t\sin(1.00 * 6.2832\ t)$	0.506	0.465	0.287	0.097	0.000	0.271
$0.1\ t\sin(2.92 * 6.2832\ t)$	0.136	0.000	0.000	0.114	0.010	0.052
$0.1\ t\sin(4.58 * 6.2832\ t)$	0.006	0.000	0.018	0.000	0.028	0.010

Table 2 shows that the maximum damage takes place if the first mode is excited when the amplitudes of the 3 excitations are the same. This is the utmost dangerous excitation for the structure. Figures 4, 6 and 8 show the excitation $\ddot{u}_g(t)$ normalized to gravitational constant g and the response of the structure in terms of relative displacements $x_i(t)$ in mm. Figures 5, 7 and 9 are the corresponding instantanous local softening values $S_i(t)$. All of these six figures and Table 2 are consistent with the mode shapes. The first mode shape leads to the fact that the first storey relative displacement should be maximum and the maximum damage should take place in the lower part of the structure, especially in the first storey when the first mode is excited. Second mode shape describes the behaviour observed in Figures 6 and 7 that the maximum damage should take place at the first and fourth storeys where the second eigenvector has big relative changes in the components. Third mode shape fits to the results presented in Figures 8 and 9 that the damage distribution follows the shape of the third eigenvector.

Table 3. Sine excitation and the modal MSDI and overall MSDI of the first type

Excitation	$\delta_{M,1}$	$\delta_{M,2}$	$\delta_{M,3}$	$\delta_{M,4}$	$\delta_{M,5}$	$\hat{\delta}_M$
$0.1\ t\sin(1.00 * 6.2832\ t)$	0.435	0.296	0.327	0.277	0.122	0.379
$0.1\ t\sin(2.92 * 6.2832\ t)$	0.068	0.089	0.036	0.042	0.034	0.067
$0.1\ t\sin(4.58 * 6.2832\ t)$	0.007	0.009	0.017	0.009	0.009	0.010

The evolution of the modal MSDI for the sine excitations are given in Figures 10, 11 and 12 and the maximum modal MSDI are tabulated in Table 3. These are calculated from

the instantaneous global stiffness matrix. From Table 3, it is clear that the sine excitations for the first, second and third modes yield maximum damages in the corresponding modes compared to the other modes. The first mode excitation is the most dangerous for the structure causing an overall modal MSDI of the first type of magnitude 0.379. The evolution of the modal MSDI is also estimated from the base acceleration and top storey displacement time series relative to the ground using a Fourier analysis, with moving time windows of length 5 sec, from the peaks of the frequency transfer function as 0.45, 0.35 and 0.30 for the first three modes in the first sine excitation. These results are close to the exact results, thus, the method can also quantify modal damage from earthquake records.

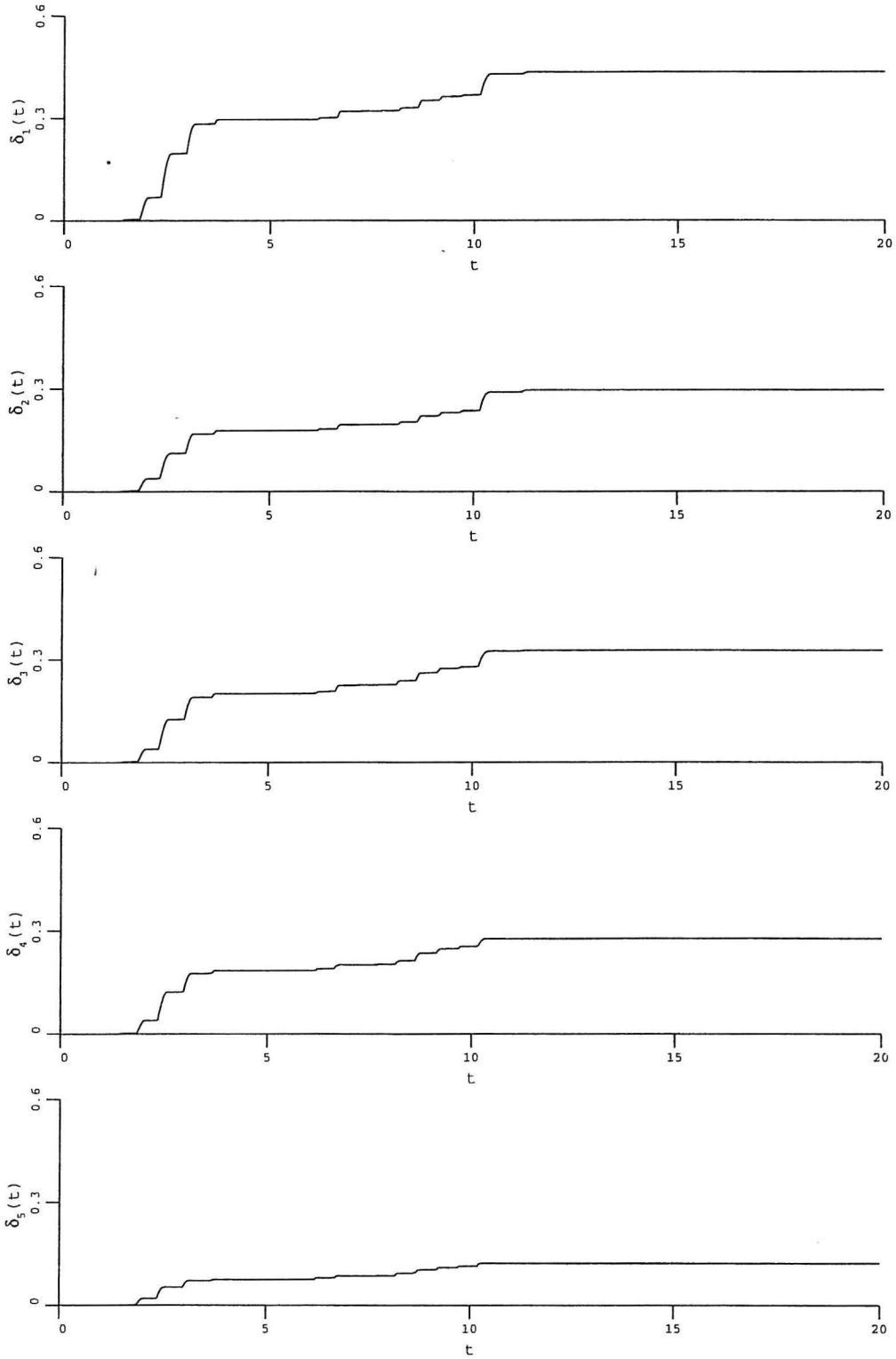

Figure 10. The evolution of the modal softening values $\delta_j(t)$ during the first sine excitation.

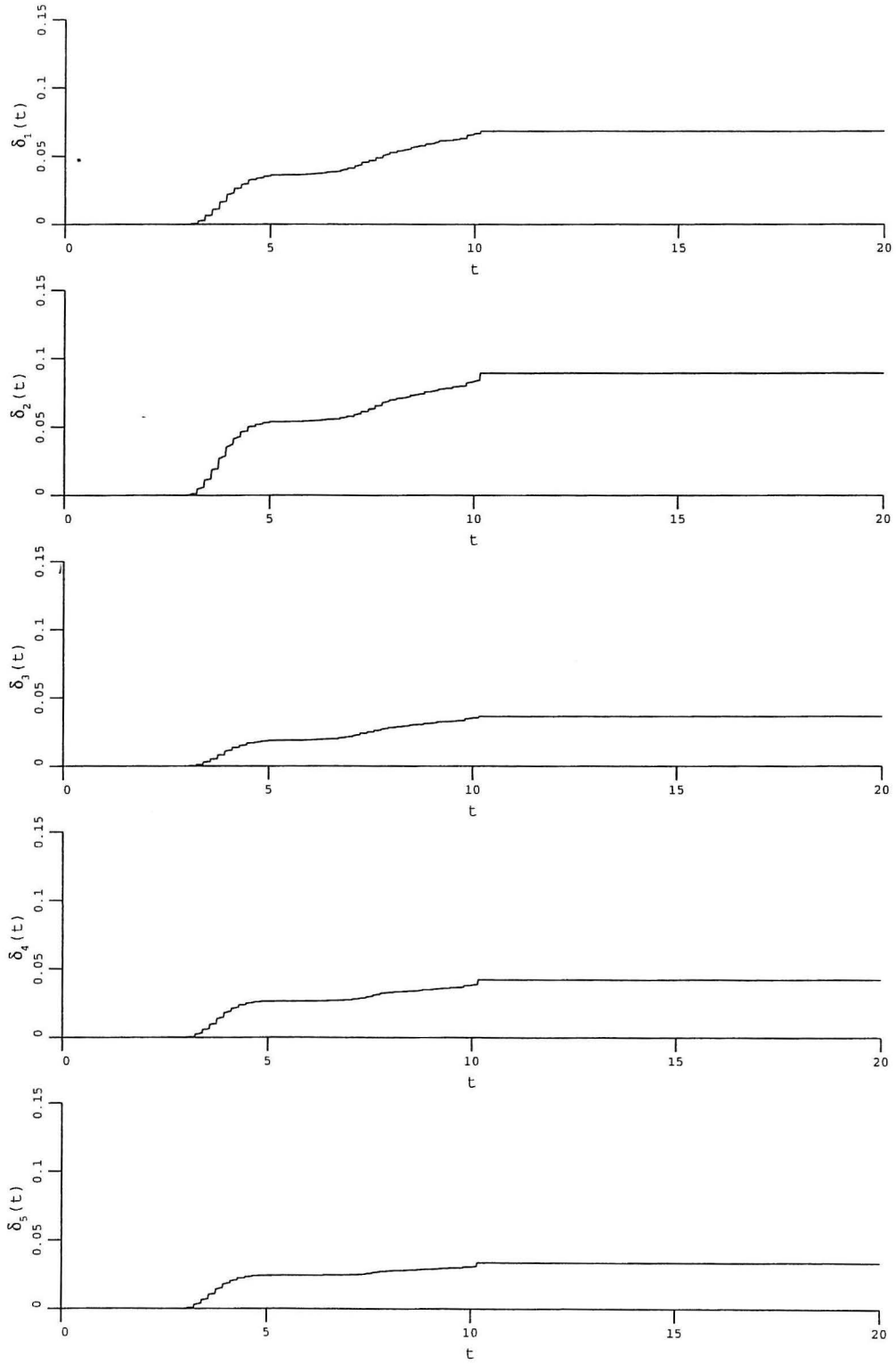

Figure 11. The evolution of the modal softening values $\delta_j(t)$ during the second sine excitation.

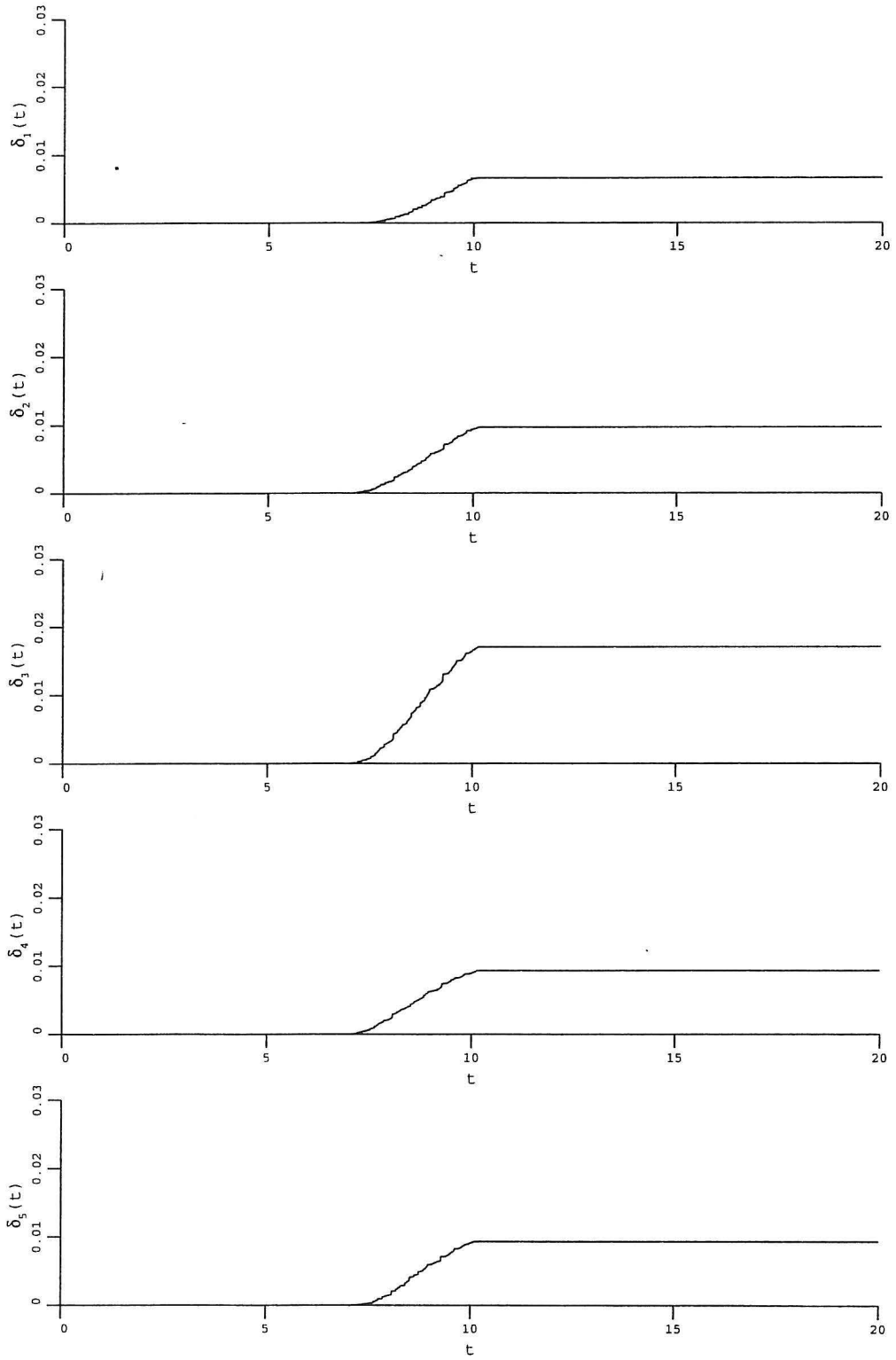

Figure 12. The evolution of the modal softening values $\delta_j(t)$ during the third sine excitation.

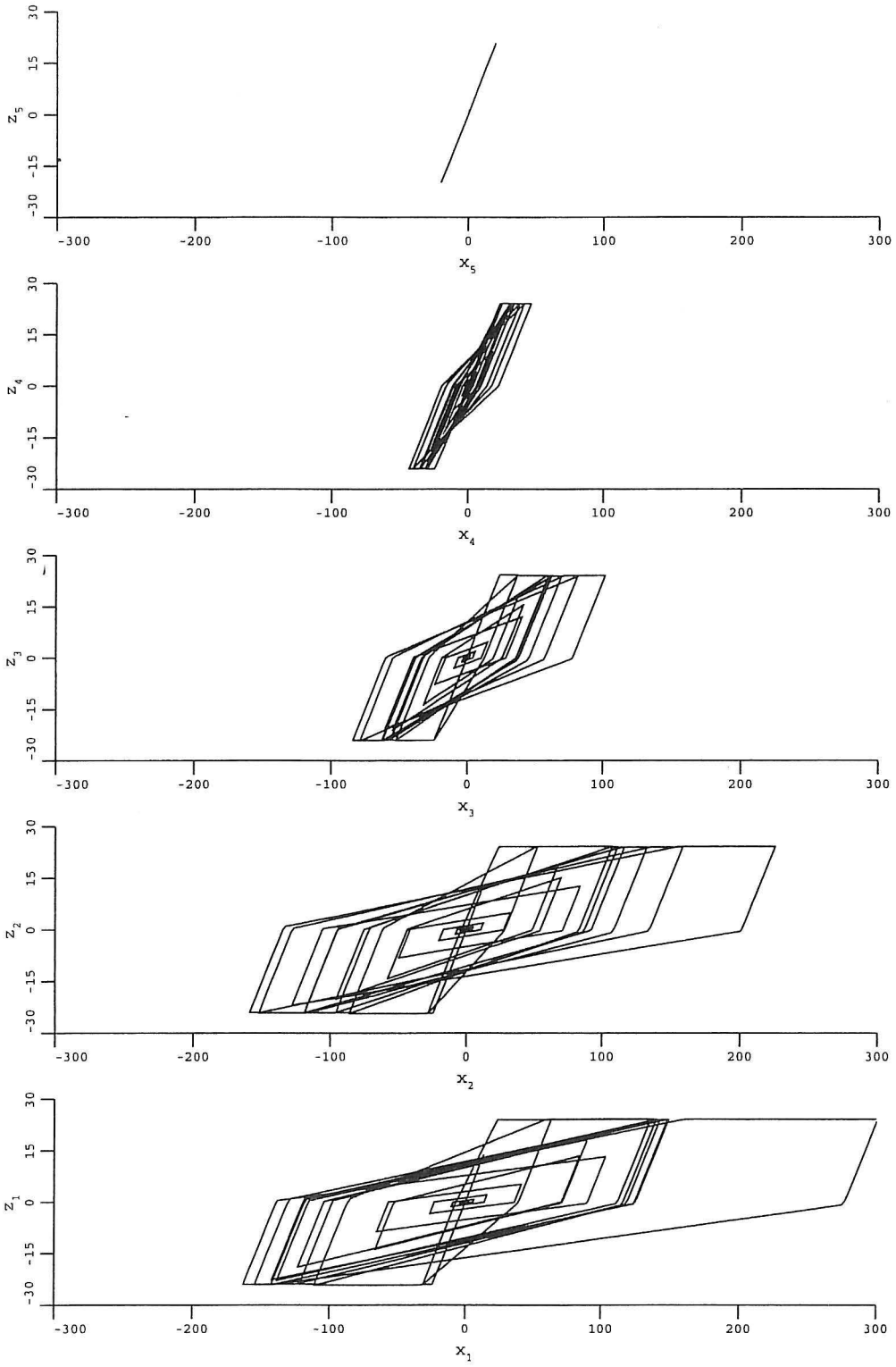

Figure 13. The hysteresis loop of x_i and z_i, $i = 1, 2, \cdots, 5$ in mm during the first sine excitation.

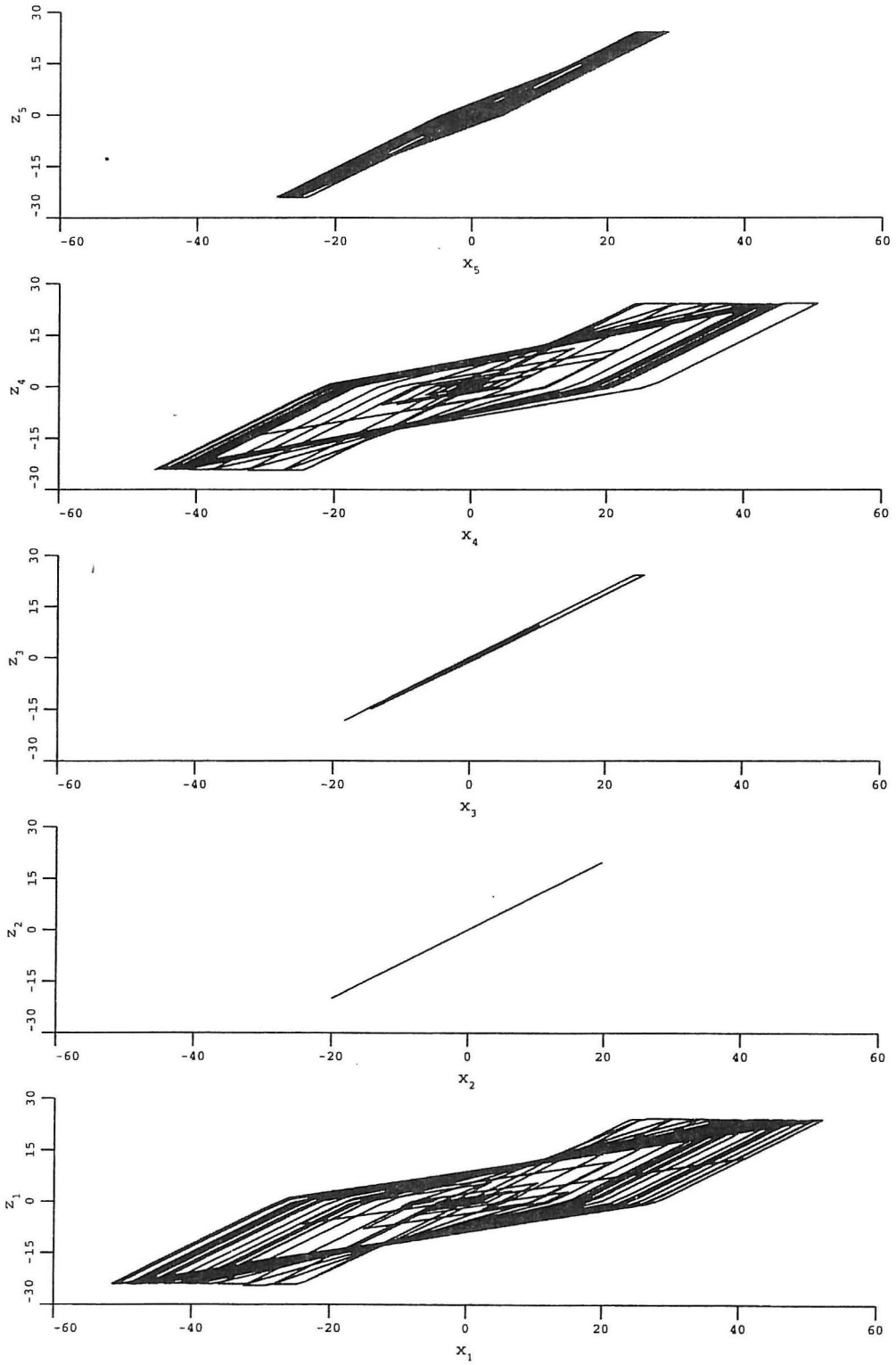

Figure 14. The hysteresis loop of x_i and z_i, $i = 1, 2, \cdots, 5$ in mm during the second sine excitation.

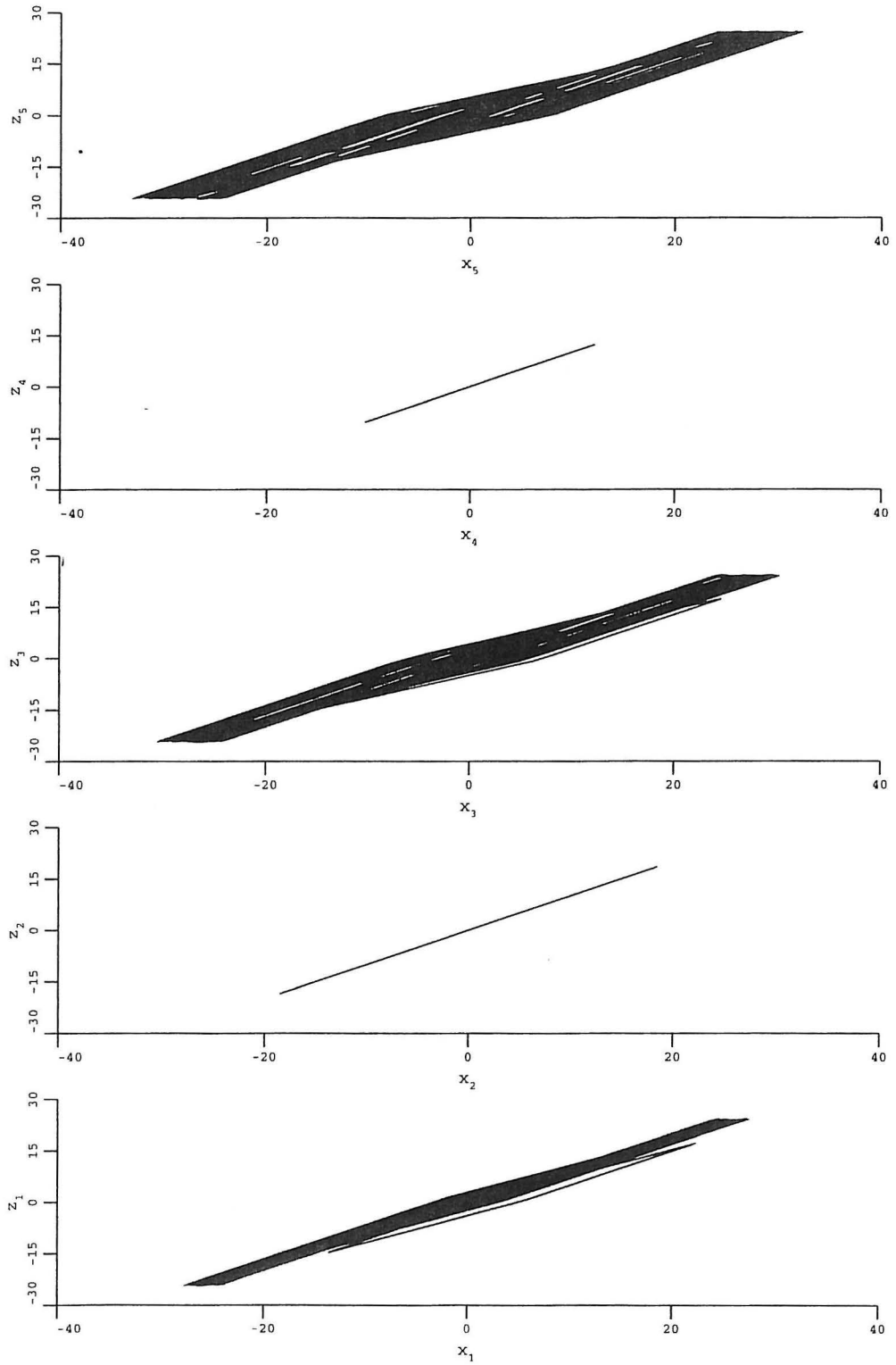

Figure 15. The hysteresis loop of x_i and z_i, $i = 1, 2, \cdots, 5$ in mm during the third sine excitation.

The hysteresis loops of x_i and z_i, $i = 1, 2, \cdots, 5$ in the first, second and third sine excitations are shown in Figures 13, 14 and 15. These are given to show the energy absorbtion in each of these ground excitations and all of these figures are consistent with the form of the mode shapes, e.g. maximum energy is absorbed in the lower part of the structure, especially in the first storey level, when the first mode is excited. This also shows that the damage models based on energy-absorbtion are highly correlated to the local MSDI based on the changes in the eigenfrequency of the local oscillators. It is concluded from the sine runs that the model is robust in the consistent quantification of damage.

Next, earthquake excitations are studied and a statistical analysis is performed to relate local and modal damage indicators. The ground excitation, $\ddot{u}_g(t)$ is modelled as a stationary stochastic Gaussian process $V(t)$ with Kanai-Tajimi spectrum multiplied by an envelope function $E(t)$.

$$\ddot{u}_g(t) = E(t)V(t) \tag{19}$$

$$E(t) = \begin{cases} c_1 t & , \quad t < t_0 \\ c_2 e^{-c_3(t-t_0)} & , \quad t > t_0 \end{cases} \tag{20}$$

$$S_{VV}(\omega) = \frac{\omega_g^4 + 4\zeta_g^2\omega_g^2\omega^2}{(\omega^2 - \omega_g^2)^2 + 4\zeta^2\omega_g^2\omega^2} S_0 \tag{21}$$

For all the earthquakes applied, $t_0 = 7$ sec, $\zeta_g = 0.3$, $S_0 = 1$ m^2 sec^4 and the other envelope and spectrum parameters ω_g, c_1, c_2, c_3 are given below for different types of earthquake simulations. It should be noted that a match in ω_g and the jth frequency of the structure denotes an earthquake exciting the jth mode the most. Three different types of ground motions with statistically equivalent energy contents are utilized for excitation purposes. These are named as Type A, B and C. The parameters for Type A are $\omega_g = 6.6$ Hertz, $c_1 = 0.005$ sec^{-1}, $c_2 = 0.035$, $c_3 = 0.2$ sec^{-1}. The parameters for Type B and C are respectively $\omega_g = 19.2$ Hertz, $c_1 = 0.00292$ sec^{-1}, $c_2 = 0.02044$, $c_3 = 0.2$ sec^{-1} and $\omega_g = 30.3$ Hertz, $c_1 = 0.00233$ sec^{-1}, $c_2 = 0.01631$, $c_3 = 0.2$ sec^{-1}. In these earthquakes Kanai-Tajimi spectrum hits to its maximum value at the first, second and third frequency of the structure respectively, thus these modes are excited the most, see Figure 16. The simulation of the stationary Gaussian stochastic processes is performed using the simulation procedure of Shinozuka and Deodatis (1991) which is based on spectral representation.

The results for one realization of three different earthquake excitations are given below. The peak accelerations in Type A, B and C earthquake simulations are $0.392g$, $0.681g$ and $0.676g$ for the shown realizations. These are strong earthquakes which may cause moderate to severe damage in RC structures.

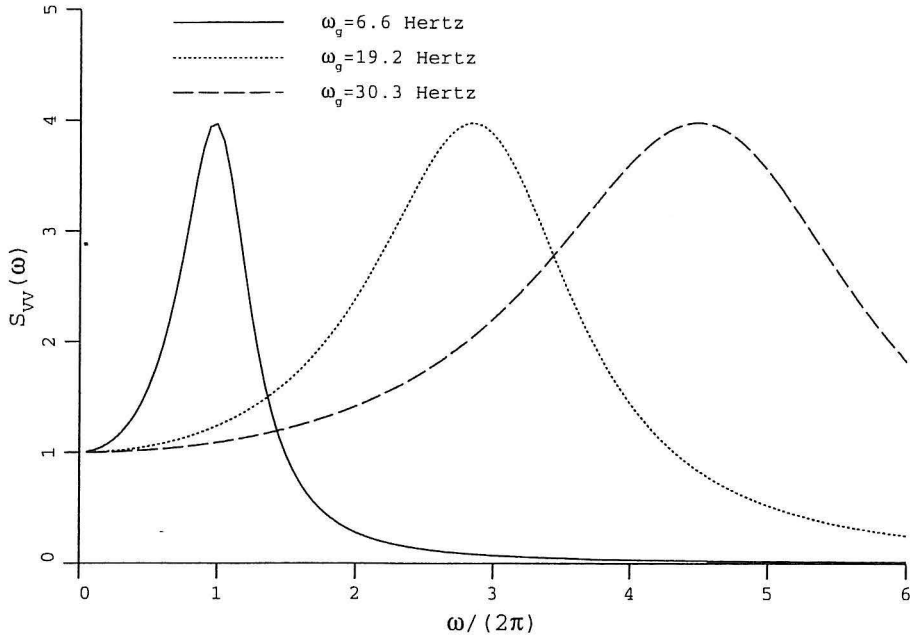

Figure 16. Kanai-Tajimi spectrum for the earthquake excitations.

Table 4. Seismic excitation and the local MSDI and overall MSDI of the second type

Earthquake excitation	$S_{M,1}$	$S_{M,2}$	$S_{M,3}$	$S_{M,4}$	$S_{M,5}$	$\hat{S}_M$
Type A ($\omega_g = 6.6$)	0.420	0.303	0.136	0.081	0.000	0.173
Type B ($\omega_g = 19.2$)	0.048	0.008	0.026	0.023	0.000	0.021
Type C ($\omega_g = 30.3$)	0.013	0.000	0.003	0.000	0.000	0.003

The earthquake excitations and the response of the structure in terms of relative displacements are shown in Figures 17, 19 and 21. Figures 18, 20 and 22 are the corresponding local MSDI values and Tables 4 and 5 are to list the local, modal and overall MSDI. All of these six figures and two tables are consistent with the excitations and mode shapes. Since Type A earthquake simulation excites the first mode the most, it causes the maximum overall damage compared to the Type B and C excitations, see Table 4 and 5, and the lower part of the structure experiences the most damage. Since Type B and C earthquake models also excite the other modes, in addition to the second and third mode, respectively, all modes are damaged and contribute to the distribution of damage in the structure. Figures 23, 24 and 25 show the exact modal MSDI. The modal MSDI values calculated form a Fourier analysis are 0.34, 0.24, 0.15 for the first three modes using Type A base excitation and top storey total displacement time series. These results are close to the exact ones, thus, the modal MSDI can always be calculated from earthquake records via a Fourier analysis. Figures 26, 27 and 28 are the the hysteresis loops of x_i and z_i in the A, B and C types of earthquake excitations where the severe damage due to Type A excitation is also implemented.

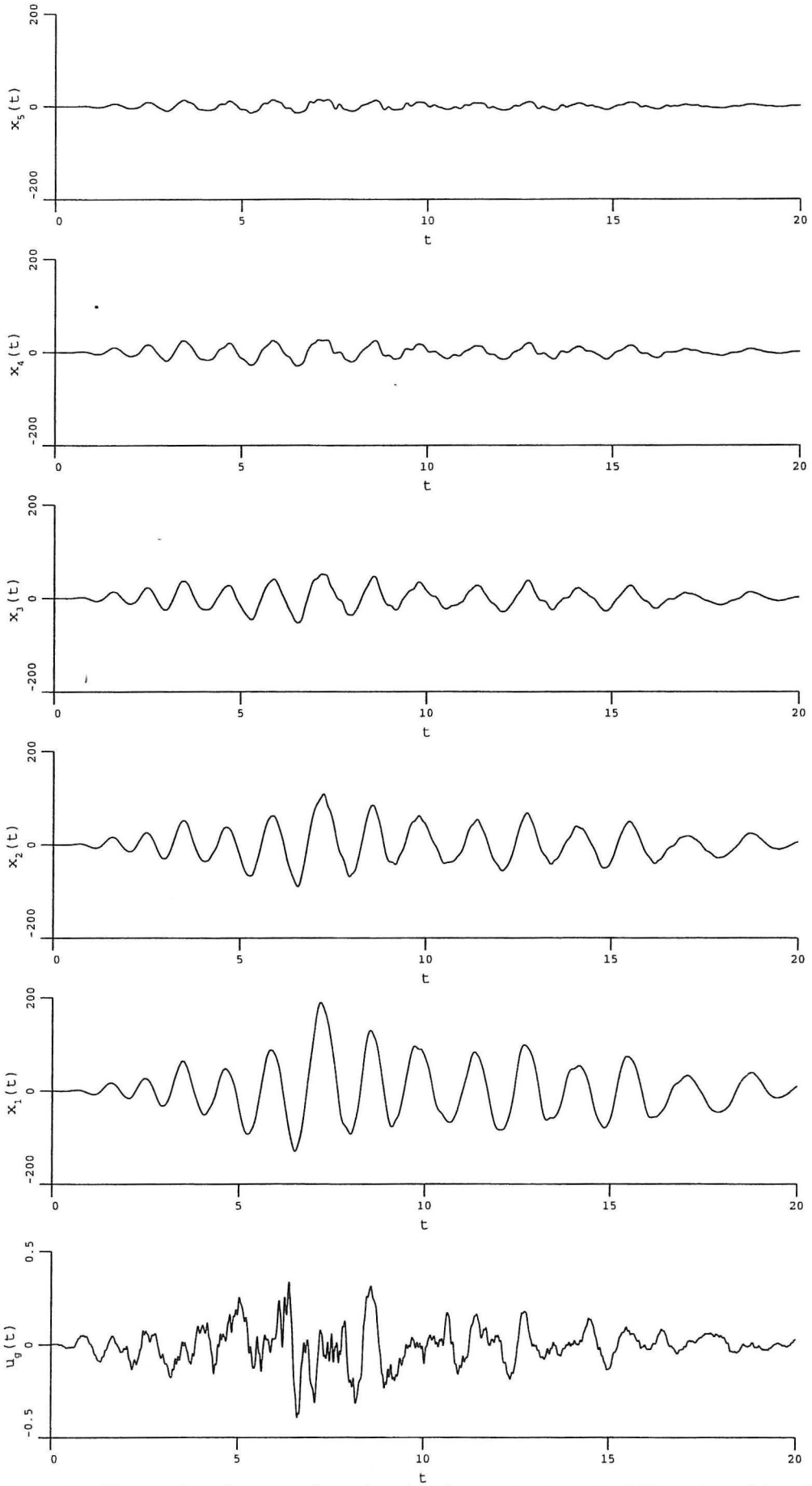

Figure 17. The earthquake ground acceleration (normalized to g) of Type A exciting the first mode and the response of the structure in terms of relative displacements $x_i(t)$ in mm.

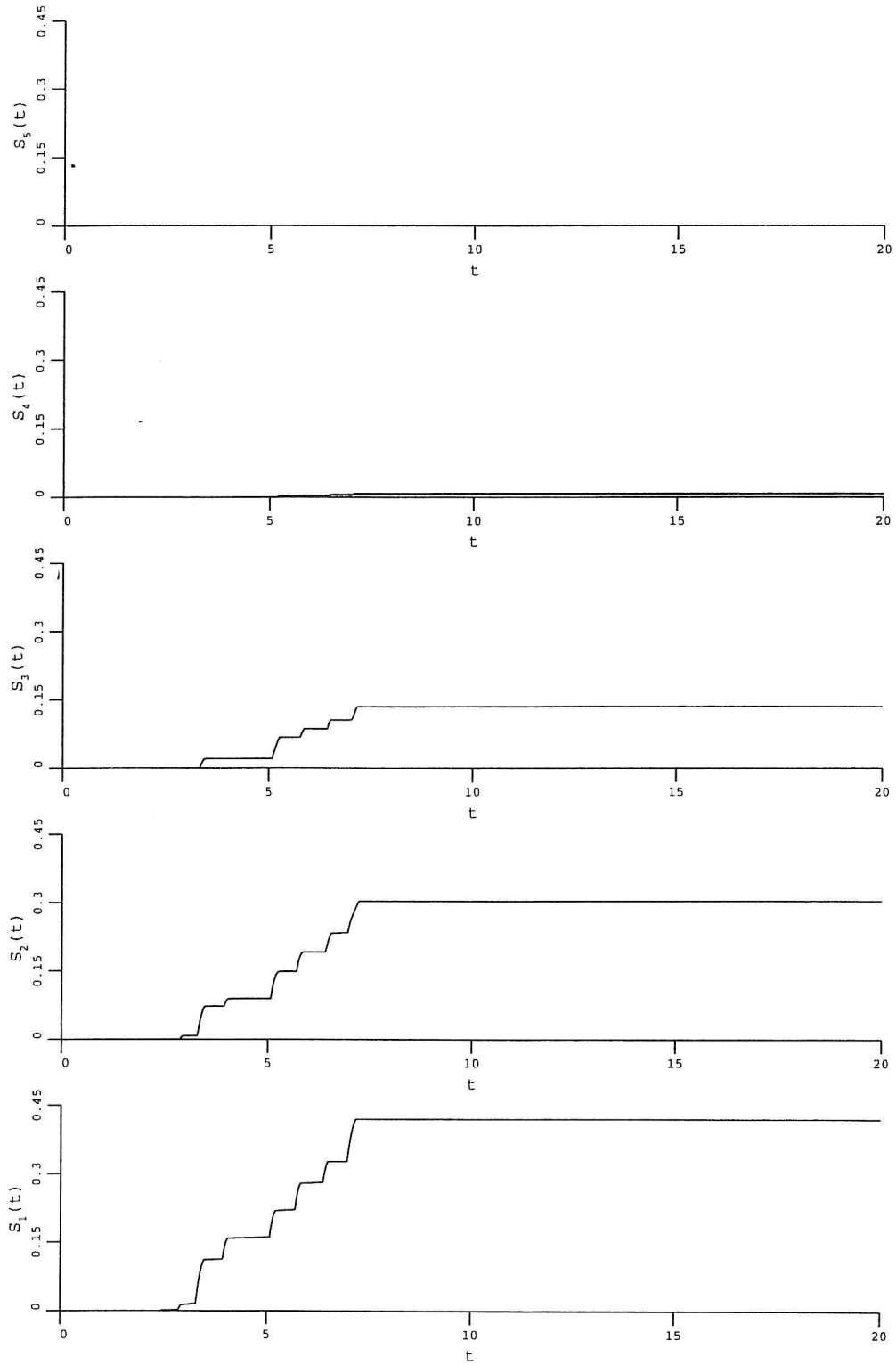

Figure 18. Instantaneous local softening values $S_i(t)$ during the Type A earthquake excitation.

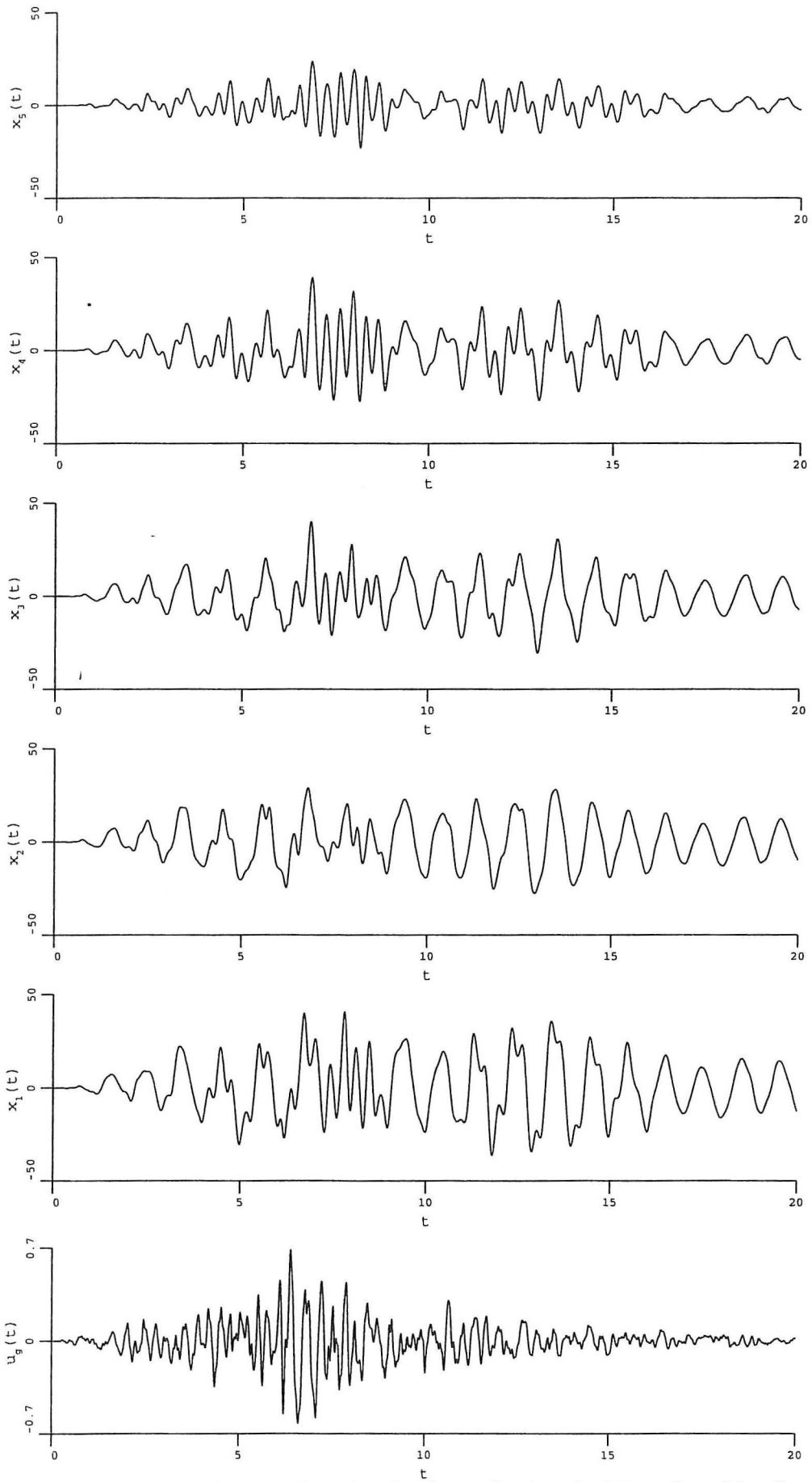

Figure 19. The earthquake ground acceleration (normalized to g) of Type B exciting the second mode and the response of the structure in terms of relative displacements $x_i(t)$ in mm.

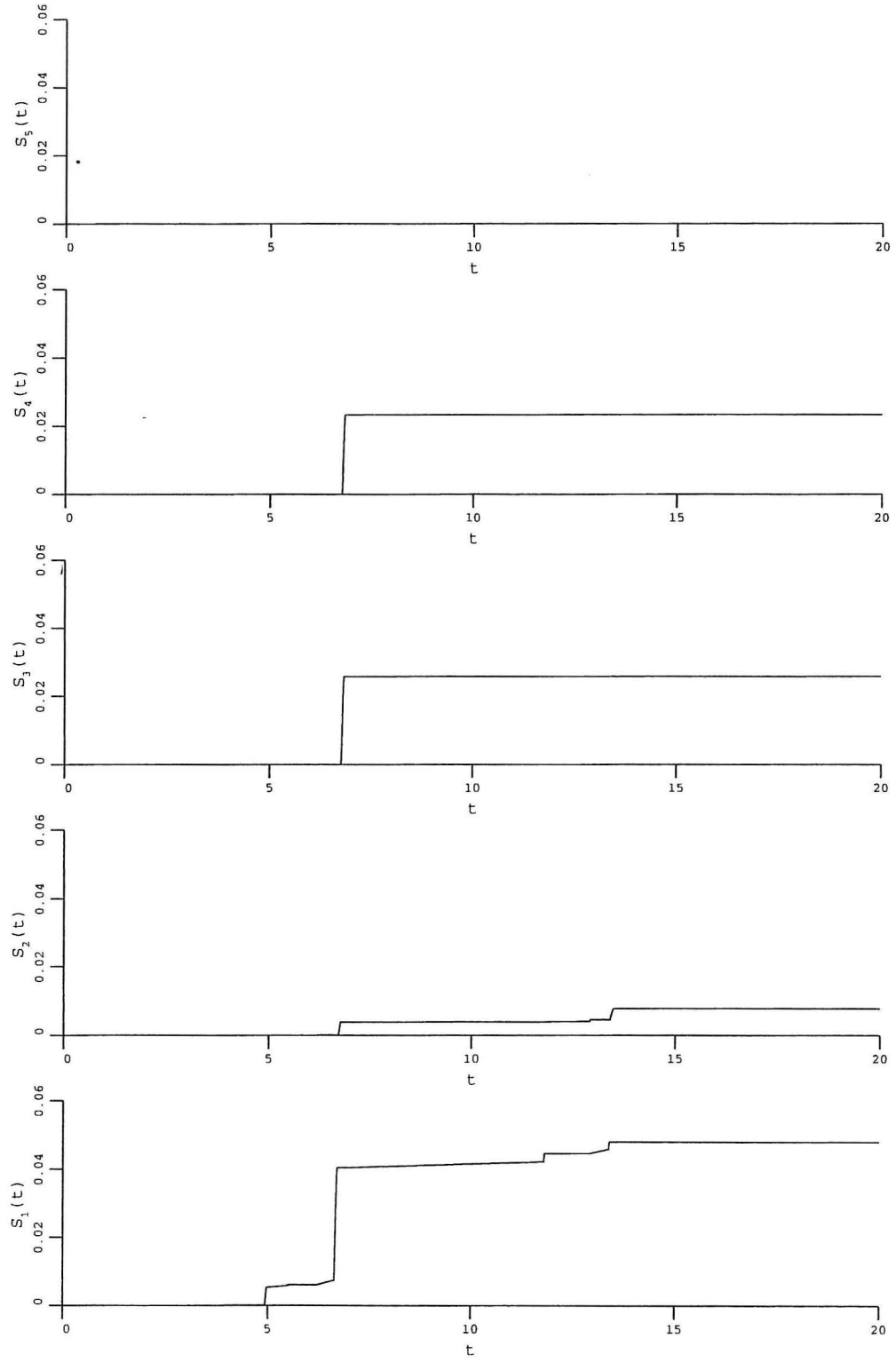

Figure 20. Instantaneous local softening values $S_i(t)$ during the Type B earthquake excitation.

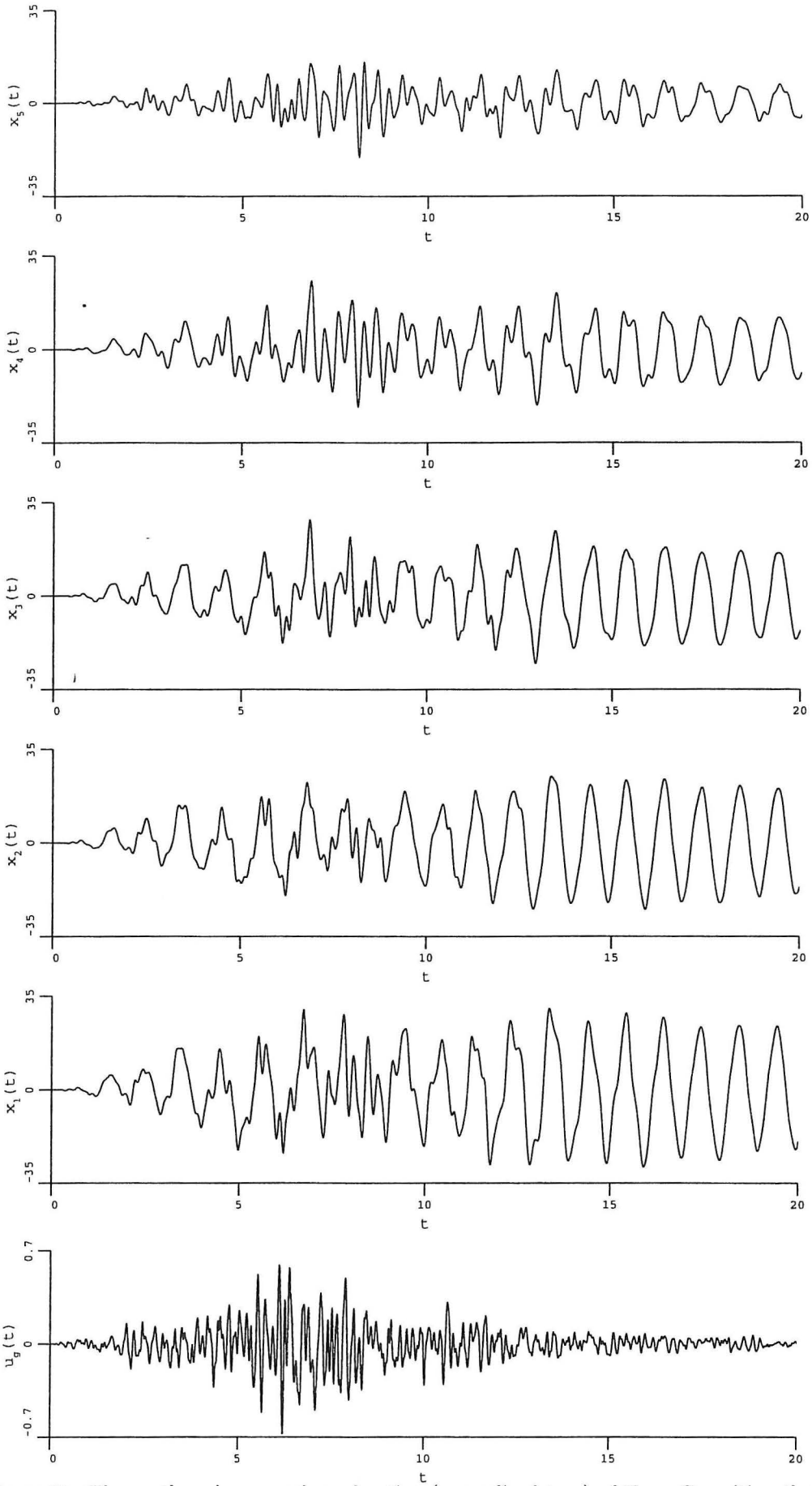

Figure 21. The earthquake ground acceleration (normalized to g) of Type C exciting the third mode and the response of the structure in terms of relative displacements $x_i(t)$ in mm.

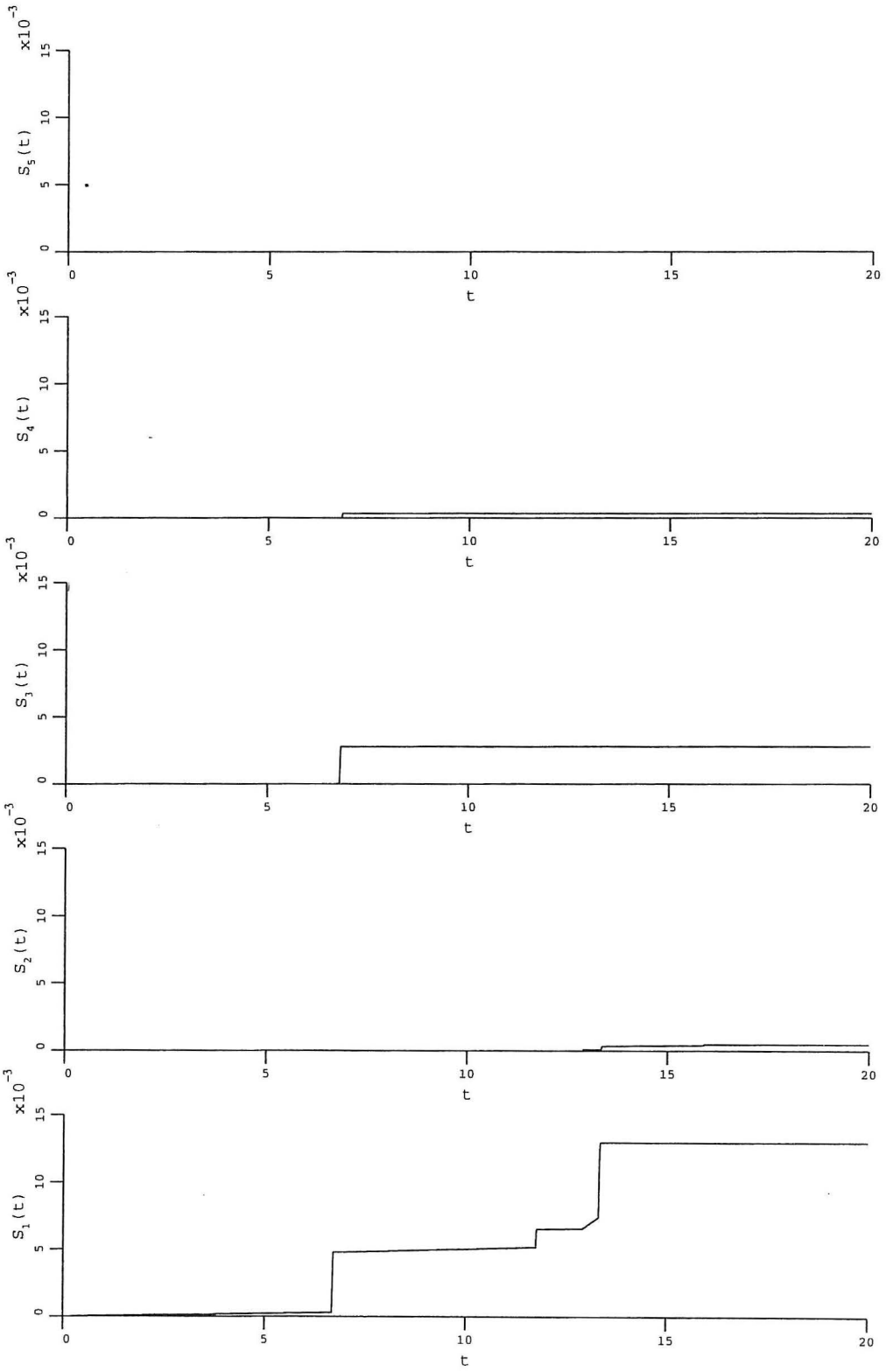

Figure 22. Instantaneous local softening values $S_i(t)$ during the Type C earthquake excitation.

Table 5. Seismic excitation and the modal MSDI and overall MSDI of the first type

Earthquake excitation	$\delta_{M,1}$	$\delta_{M,2}$	$\delta_{M,3}$	$\delta_{M,4}$	$\delta_{M,5}$	$\hat{\delta}_M$
Type A ($\omega_g = 6.6$)	0.314	0.186	0.201	0.170	0.063	0.262
Type B ($\omega_g = 19.2$)	0.028	0.026	0.019	0.013	0.019	0.026
Type C ($\omega_g = 30.3$)	0.005	0.004	0.004	0.002	0.002	0.005

A statistical analysis based on Monte Carlo simulations is performed to study the means, coefficient of variations of the local, modal and overall MSDI and the correlations among them.

30 realizations of the earthquake time series are generated, the local, modal and overall MSDI values due to these 30 realizations are computed and the relationships between local and modal MSDI are investigated. The mean values and coefficient of variations are tabulated below in Tables 6 and 7 for three different types of earthquakes which have the same parameters with the ones listed above. As seen in Tables 6 and 7, the means of the local damages after 30 realizations of Type A earthquake are consitent with the first mode shape and the mean of the overall MSDI values of the first or second kinds indicate that Type A earthquake would cause the most damage in the structure compared to Type B and C earthquakes. It should be noted that in the studied shear frame with equal storey stiffness, the top storey columns did not experience any damage. The coefficient of variation in the Type A earthquakes are observed to be relatively small compared to Type B and C earthquakes. This shows that the reliability models can estimate small and sharper confidence intervals for severe damage compared to light damage. This conclusion supports the findings of Hassiotis and Jeong (1993) about the polluted data analysis that the light damage cannot be predicted accurately from the polluted data.

The correlation matrices for the corresponding cases are given in Tables 8, 9 and 10. The seventh column of Table 8 shows that the numerical correlations between $\delta_{M,1}$ and $S_{M,i}$ are consistent with the first mode shape; there is higher correlation with the damage in the lower storeys and $\delta_{M,1}$ compared to higher storeys. The correlations among modal MSDI increase when more modes are excited. This can be seen when the correlations in Tables 8, 9 and 10 are compared. Type C earthquake, which yields the results of Table 10, excites almost all the five modes, mode 3 the most, thus the correlations among δ_j are higher in table 10 compared to Tables 8 and 9. Overall MSDI $\hat{\delta}_M$ and $\hat{S}_M$ are highly correlated in all cases, correlations being 0.995, 0.919, 0.984. This shows that any of these two indicators can be used as a scalar value to average the overall damage.

Table 6. The mean and coefficient of variation of the local MSDI and overall MSDI of the second type in 30 simulations

Earthquake type	$S_{M,1}$	$S_{M,2}$	$S_{M,3}$	$S_{M,4}$	$S_{M,5}$	$\hat{S}_M$
Type A ($w_g = 6.6$)	0.449, 0.165	0.361, 0.192	0.196, 0.246	0.035, 0.492	0.000, -	0.208, 0.189
Type B ($w_g = 19.2$)	0.167, 0.397	0.090, 0.634	0.056, 0.743	0.024, 0.767	0.000, -	0.068, 0.447
Type C ($w_g = 30.3$)	0.105, 0.543	0.055, 0.732	0.023, 1.075	0.003, 1.850	0.000, -	0.037, 0.625

Table 7. The mean and coefficient of variation of the modal MSDI and overall MSDI of the first type in 30 simulations

Earthquake type	$\delta_{M,1}$	$\delta_{M,2}$	$\delta_{M,3}$	$\delta_{M,4}$	$\delta_{M,5}$	$\hat{\delta}_M$
Type A ($w_g = 6.6$)	0.354, 0.197	0.223, 0.234	0.240, 0.222	0.206, 0.181	0.083, 0.174	0.301, 0.203
Type B ($w_g = 19.2$)	0.109, 0.439	0.073, 0.389	0.067, 0.476	0.061, 0.543	0.040, 0.498	0.093, 0.434
Type C ($w_g = 30.3$)	0.063, 0.604	0.039, 0.590	0.037, 0.639	0.034, 0.693	0.019, 0.750	0.053, 0.607

Table 8. The correlation between the local, modal and overall MSDI for earthquake type A with $w_g = 6.6$, $c_1, c_2, c_3 = 0.005, 0.035, 0.2$.

	$S_{M,1}$	$S_{M,2}$	$S_{M,3}$	$S_{M,4}$	$S_{M,5}$	$\hat{S}_M$	$\delta_{M,1}$	$\delta_{M,2}$	$\delta_{M,3}$	$\delta_{M,4}$	$\delta_{M,5}$	$\hat{\delta}_M$
$S_{M,1}$	1.000	0.937	0.764	0.525	-	0.939	0.946	0.920	0.907	0.789	0.579	0.936
$S_{M,2}$		1.000	0.927	0.724	-	0.995	0.916	0.914	0.922	0.877	0.724	0.919
$S_{M,3}$			1.000	0.897	-	0.937	0.768	0.801	0.812	0.855	0.808	0.785
$S_{M,4}$				1.000	-	0.759	0.556	0.616	0.620	0.724	0.831	0.583
$S_{M,5}$					-	-	-	-	-	-	-	-
$\hat{S}_M$						1.000	0.916	0.918	0.919	0.878	0.743	0.919
$\delta_{M,1}$							1.000	0.993	0.990	0.920	0.755	0.999
$\delta_{M,2}$								1.000	0.995	0.947	0.811	0.997
$\delta_{M,3}$									1.000	0.963	0.826	0.995
$\delta_{M,4}$										1.000	0.935	0.936
$\delta_{M,5}$											1.000	0.783
$\hat{\delta}_M$												1.000

Table 9. The correlation between the local, modal and overall MSDI for earthquake type B with $w_g = 19.2$, $c_1, c_2, c_3 = 0.00292, 0.02044, 0.2$.

	$S_{M,1}$	$S_{M,2}$	$S_{M,3}$	$S_{M,4}$	$S_{M,5}$	$\hat{S}_M$	$\delta_{M,1}$	$\delta_{M,2}$	$\delta_{M,3}$	$\delta_{M,4}$	$\delta_{M,5}$	$\hat{\delta}_M$
$S_{M,1}$	1.000	0.824	0.492	-0.091	-	0.876	0.945	0.915	0.879	0.810	0.551	0.934
$S_{M,2}$		1.000	0.741	0.008	-	0.945	0.941	0.865	0.956	0.980	0.738	0.941
$S_{M,3}$			1.000	0.505	-	0.834	0.712	0.765	0.822	0.832	0.964	0.744
$S_{M,4}$				1.000	-	0.226	0.052	0.275	0.173	0.163	0.599	0.105
$S_{M,5}$					-	-	-	-	-	-	-	-
$\hat{S}_M$						1.000	0.974	0.974	0.996	0.976	0.861	0.984
$\delta_{M,1}$							1.000	0.966	0.983	0.951	0.731	0.998
$\delta_{M,2}$								1.000	0.965	0.914	0.817	0.976
$\delta_{M,3}$									1.000	0.983	0.831	0.990
$\delta_{M,4}$										1.000	0.824	0.959
$\delta_{M,5}$											1.000	0.766
$\hat{\delta}_M$												1.000

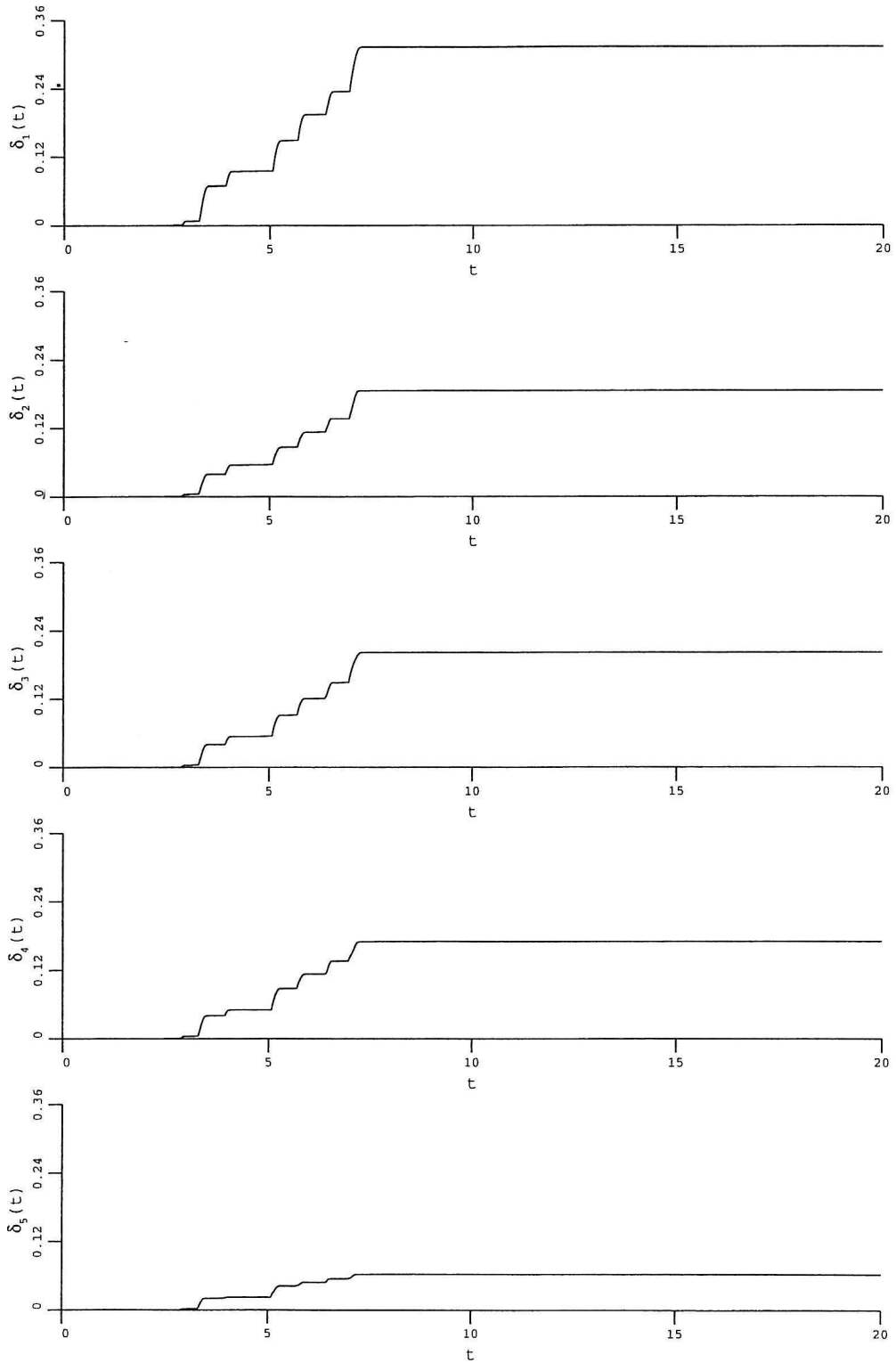

Figure 23. The evolution of the modal softening values $\delta_j(t)$ during the Type A earthquake excitation.

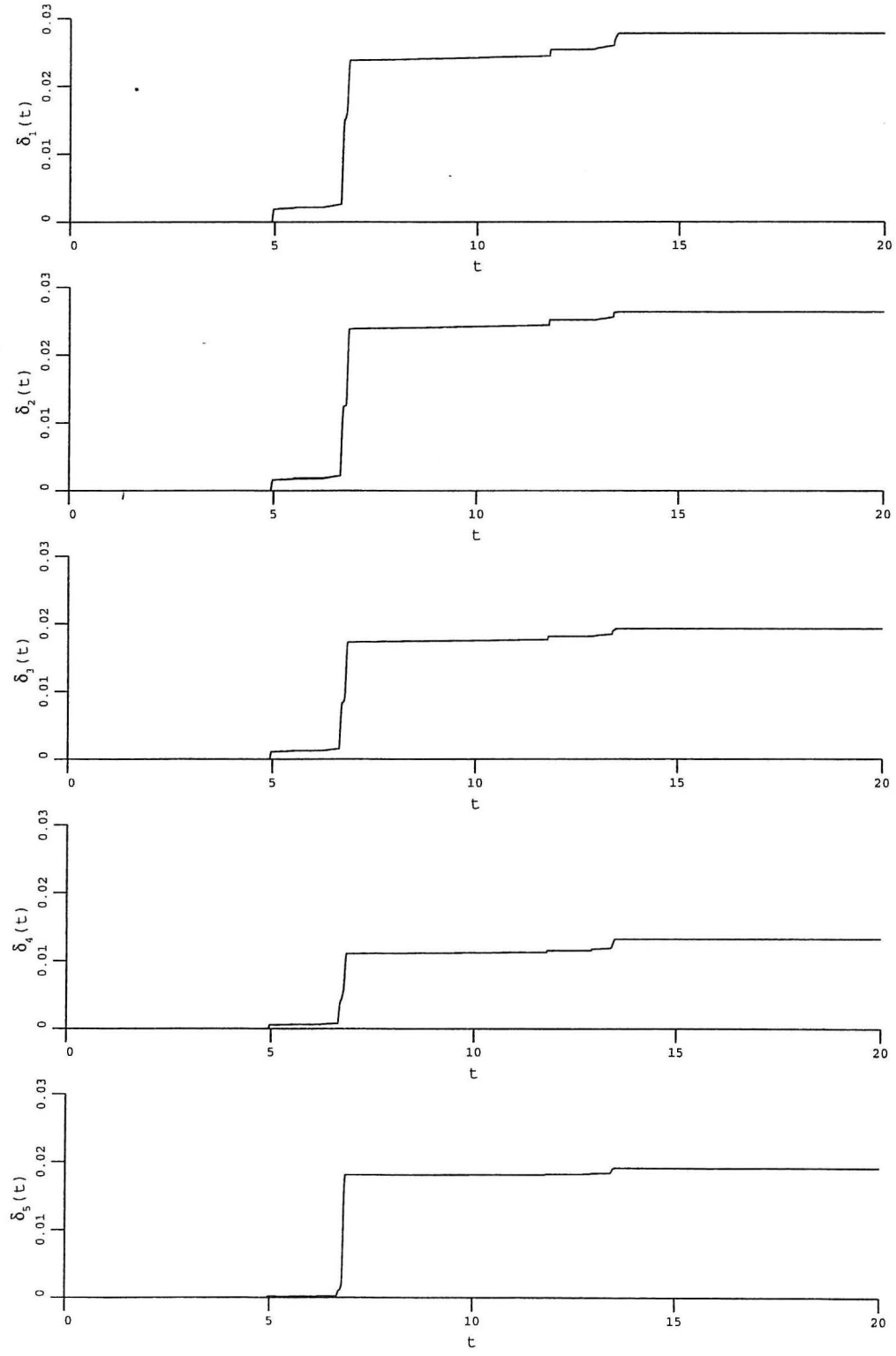

Figure 24. The evolution of the modal softening values $\delta_j(t)$ during the Type B earthquake excitation.

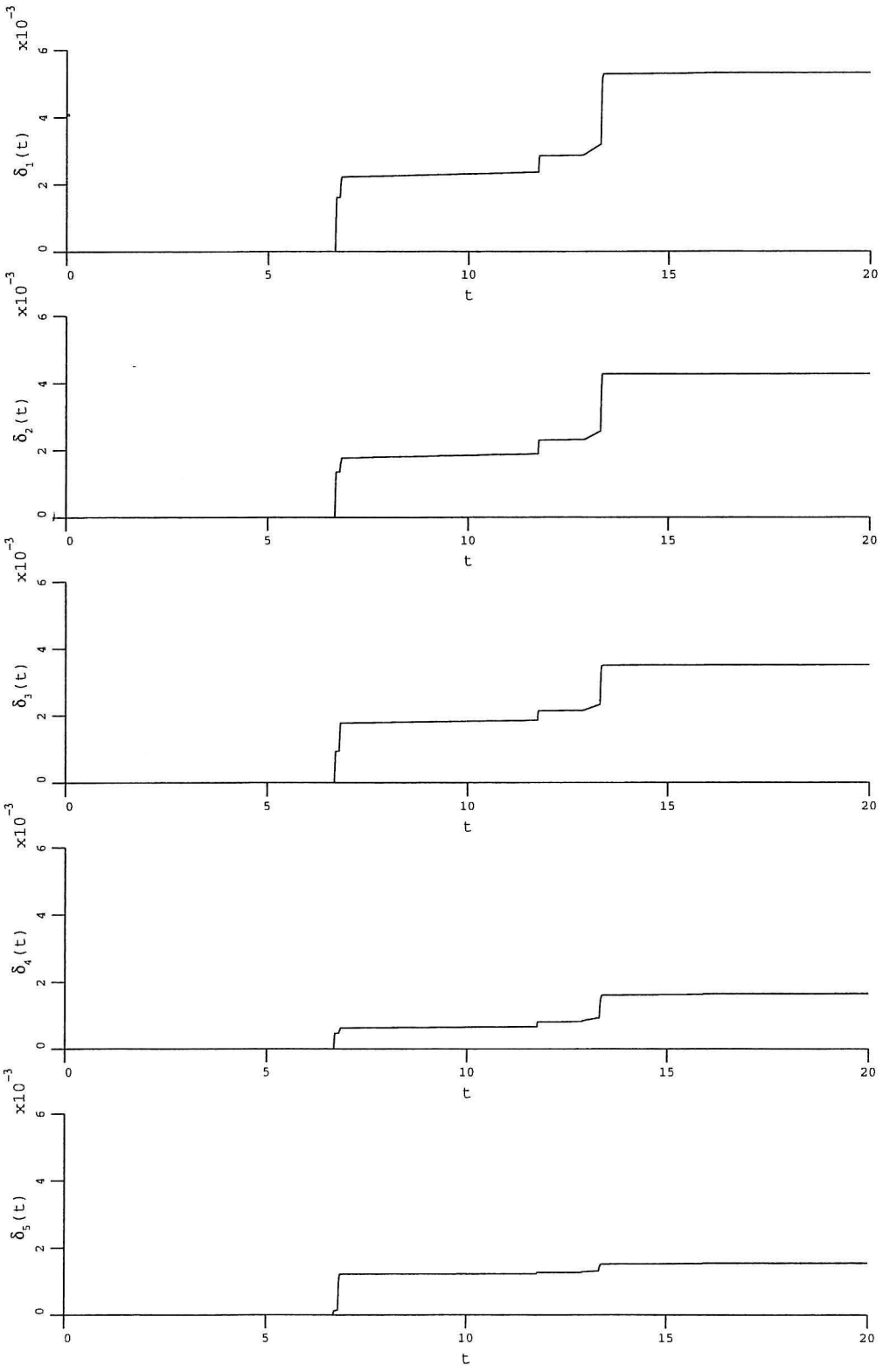

Figure 25. The evolution of the modal softening values $\delta_j(t)$ during the Type C earthquake excitation.

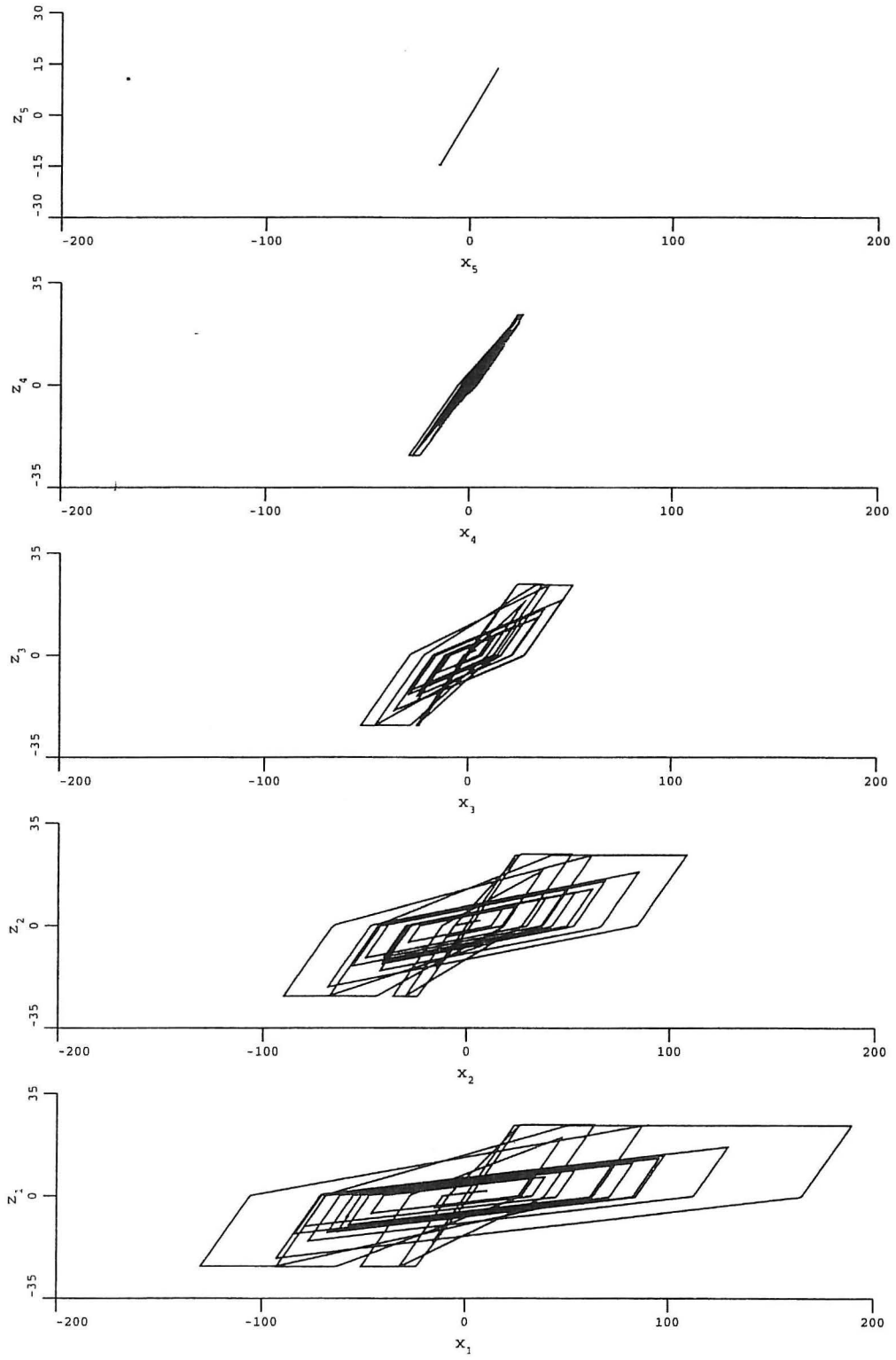

Figure 26. The hysteresis loop of x_i and z_i, $i = 1, 2, \cdots, 5$ in mm during the Type A earthquake excitation.

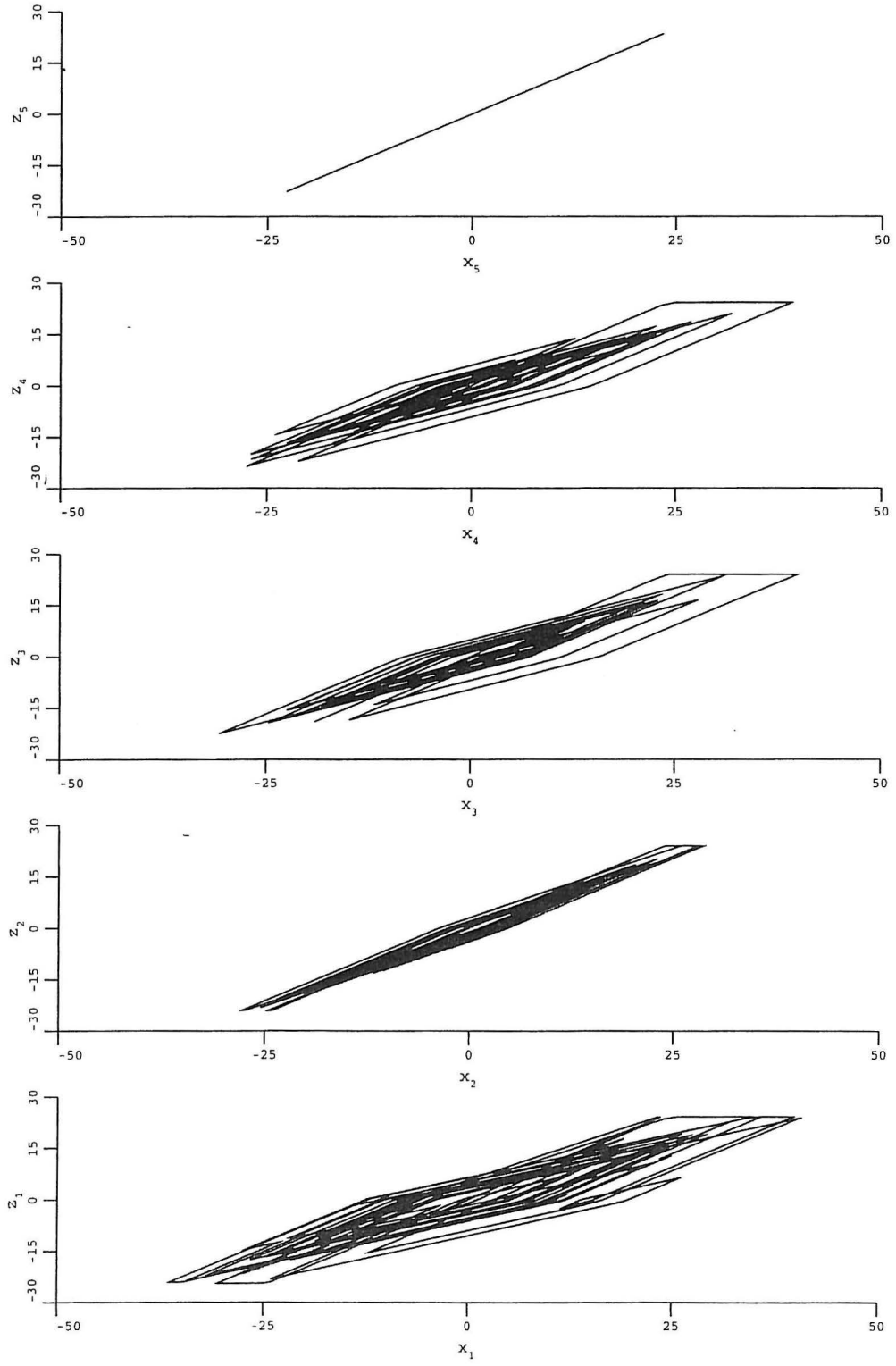

Figure 27. The hysteresis loop of x_i and z_i, $i = 1, 2, \cdots, 5$ in mm during the Type B earthquake excitation.

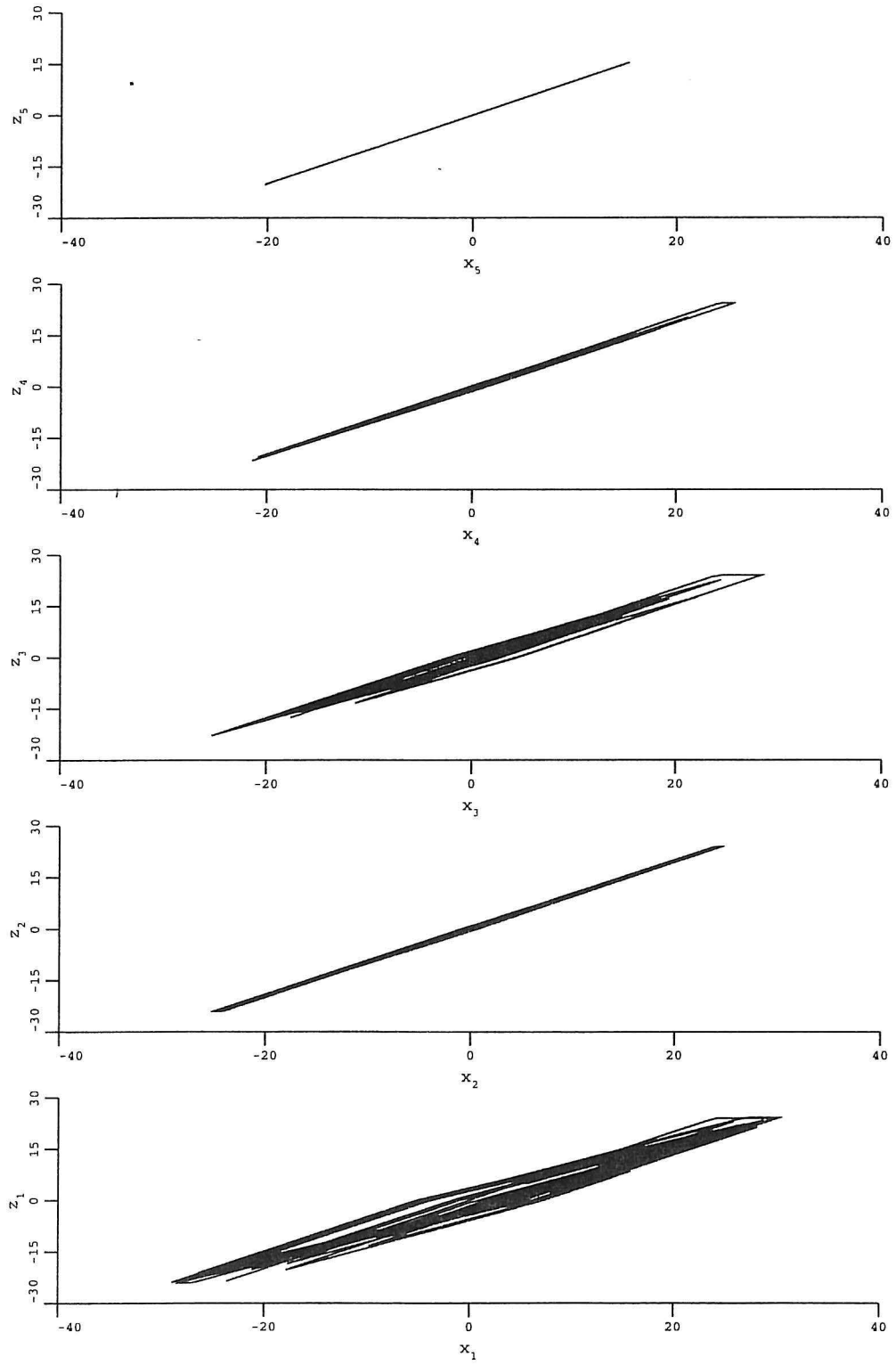

Figure 28. The hysteresis loop of x_i and z_i, $i = 1, 2, \cdots, 5$ in mm during the Type C earthquake excitation.

Table 10. The correlation between the local, modal and overall MSDI for earthquake type C with $w_g = 30.3$, $c_1, c_2, c_3 = 0.00233, 0.01631, 0.2$.

	$S_{M,1}$	$S_{M,2}$	$S_{M,3}$	$S_{M,4}$	$S_{M,5}$	$\hat{S}_M$	$\delta_{M,1}$	$\delta_{M,2}$	$\delta_{M,3}$	$\delta_{M,4}$	$\delta_{M,5}$	$\hat{\delta}_M$
$S_{M,1}$	1.000	0.840	0.662	0.390	-	0.940	0.971	0.978	0.942	0.885	0.971	0.968
$S_{M,2}$		1.000	0.823	0.458	-	0.954	0.939	0.885	0.954	0.988	0.920	0.938
$S_{M,3}$			1.000	0.732	-	0.858	0.797	0.794	0.856	0.869	0.965	0.809
$S_{M,4}$				1.000	-	0.558	0.486	0.549	0.544	0.541	0.708	0.506
$S_{M,5}$					-	-	-	-	-	-	-	-
$\hat{S}_M$						1.000	0.993	0.981	0.999	0.986	0.946	0.995
$\delta_{M,1}$							1.000	0.989	0.994	0.970	0.903	1.000
$\delta_{M,2}$								1.000	0.981	0.938	0.891	0.991
$\delta_{M,3}$									1.000	0.986	0.942	0.996
$\delta_{M,4}$										1.000	0.953	0.972
$\delta_{M,5}$											1.000	0.911
$\hat{\delta}_M$												1.000

8. CONCLUSIONS

A hysteretic mechanical formulation to quantify local, modal and overall damage in reinforced concrete shear frames subject to earthquakes is derived. Each storey of the shear frame is represented by a Clough and Johnston hysteretic oscillator with degrading elastic fraction of the restoring force. The local maximum softening damage indicators are defined based on the variation of the eigenfrequency of the local oscillators due to the local stiffness and strength deterioration. The modal maximum softening damage indicators are calculated from the variation of the eigenfrequencies of the structure during the excitation. The performance of the model is illustrated on a sample 5 storey shear frame subject to sinusoidal and simulated earthquake excitations. It is concluded that the proposed local and modal damage indicators are robust in quantifying the damage and explaining the relationships between the frequency content of the excitation and the distribution of damage in the structure.

Next, a Monte Carlo analysis is performed where the shear frame is subject to 30 independent simulations of the earthquake excitation. The resulting sample set is analyzed to determine the relationship between local and modal damage indices statistically. It is observed that, primarily, the ground excitations exciting the first mode causes severe damage to the RC structure and that the damage in the lower part of the structure is very highly correlated to the modal damage indicator of the first mode.

9. ACKNOWLEDGEMENT

The present research was partially supported by The danish Technical Research Council within the project entitled " Dynamics of Structures ".

10. REFERENCES

1. Clough, W. and Johnston, S.B. (1966) 'Effect of Stiffness Degradation on Earthquake Ductility Requirements', *Proc. 2nd Japan Earthquake Symposium* 227-232.

2. Çeçen, H. (1979) 'Response of Ten Storey, Reinforced Concrete Model Frames to Simulated Earthquakes', Ph.D. thesis, University of Illinois at Urbana Champaign.

3. DiPasquale, E. and Çakmak, A.Ş. (1990) 'Detection of Seismic Structural Damage Using Parameter-based Global Damage Indices', *Probabilistic Engineering Mechanics* **5**, 60-65.

4. Hajela, P. and Soeiro (1990) 'Structural Damage detection Based on Static and Modal Analysis', *AIAA Journal*, **28**, 1110-1115.

5. Hassiotis, S. and Jeong, G.D. (1993) 'Assesment of Structural Damage from Natural Frequency Measurements', *Computers and Structures*, **49**, 679-691.

6. Healey, T.J. and Sözen, M.A. (1978) 'Experimental Study of the Dynamic Response of a Ten Storey Reinforced Concrete with a Tail First Storey', Report No. UILU-ENG-78-2012, University of Illinois at Urbana Champaign.

7. Köylüoğlu, H.U., Nielsen, S.R.K. and Çakmak, A.Ş. (1994) 'Prediction of Global and Localized Damage and Future Reliability for RC Structures subject to Earthquakes', University of Aalborg, Structural Reliability Theory Paper No. 128, ISSN 0902-7513 R9426. Submitted to Earthquake Engineering and Structural Dynamics.

8. Minai, R. and Suzuki, Y. (1985), 'Seismic Reliability Analysis of Building Structures', *Proc. ROC-Japan joint seminar on Multiple Hazards Mitigation*, National Taiwan University, Taiwan, ROC, March 1985, 193-207.

9. Mullen, C., Micaletti, R.C. and Çakmak, A.Ş. (1995) 'A Simple Method for Estimating the Maximum Softening Damage Index', *Soil Dynamics and Earthquake Engineering VII*, Ed.: Çakmak, A. Ş. and Brebbia, C.A., 371-378, Computational Mechanics Publications, Southampton, UK.

10. Rahman, S. and Grigoriu, M. (1994), 'Local and Models for nonlinear Dynamic Analysis of Multi-Story Shear Buildings subject to Earthquakes', *Computers and Structures*, **53**, 739-754.

11. Nielsen, S.R.K. and Çakmak, A. Ş. (1992) 'Evaluation of Maximum Softening as a Damage Indicator for Reinforced Concrete under Seismic Excitation', *Proc. First Int. Con. on Computational Stochastic Mechanics*, eds: Spanos and Brebbia, 169-184.

12. Nielsen, S.R.K., Köylüoğlu, H.U. and Çakmak, A. Ş. (1993), 'One and Two Dimensional Maximum Softening Damage Indicators for Reinforced Concrete Structures under Seismic Excitation', *Soil Dynamics and Earthquake Engineering*, **11**, 435-443.

13. Nielsen, S.R.K., Skjarbek, P.S., Köylüoğlu, H.U. and Çakmak, A. Ş. (1995), 'Prediction of Global Damage and Reliability Based upon Sequential Identification and

Updating of RC Structures subject to Earthquakes' *Soil Dynamics and Earthquake Engineering VII*, Ed.: Çakmak, A. Ş. and Brebbia, C.A., 361-369, Computational Mechanics Publications, Southampton, UK.

14. Shinozuka, M. and Deodatis, G. (1991) ' Simulation of Stochastic Processes by Spectral Representation', *Applied Mechanics Reviews*, **40**, 191-204.

STRUCTURAL RELIABILITY THEORY SERIES

PAPER NO 117: H. U. Köylüoğlu, S. R. K. Nielsen & A. Ş. Çakmak: *Perturbation Solutions for Random Linear Structural Systems subject to Random Excitation using Stochastic Differential Equations.* ISSN 0902-7513 R9425.

PAPER NO. 118: I. Enevoldsen & J. D. Sørensen: *Reliability-Based Optimization in Structural Engineering.* ISSN 0902-7513 R9332.

PAPER NO. 119: I. Enevoldsen & K. J. Mørk: *Effects of a Vibration Mass Damper in a Wind Turbine Tower.* ISSN 0902-7513 R9334.

PAPER NO. 120: C. Pedersen & P. Thoft-Christensen: *Interactive Quasi-Newton Optimization Algorithms.* ISSN 0902-7513 R9346.

PAPER NO. 121: H. U. Köylüoğlu, S. R. K. Nielsen & A. Ş. Çakmak: *Applications of Interval Mapping for Structural Uncertainties and Pattern Loadings.* ISSN 0902-7513 R9411.

PAPER NO. 122: H. U. Köylüoğlu, S. R. K. Nielsen & A. Ş. Çakmak: *Fast Cell-to-Cell Mapping (Path Integration) with Probability Tails for the Random Vibration of Nonlinear and Hysteretic Systems.* ISSN 0902-7513 R9410.

PAPER NO. 123: A. Aşkar, H. U. Köylüoğlu, S. R. K. Nielsen & A. Ş. Çakmak: *Faster Simulation Methods for the Nonstationary Random Vibrations of Nonlinear MDOF Systems.* ISSN 0902-7513 R9405.

PAPER NO. 125: H. I. Hansen, P. H. Kirkegaard & S. R. K. Nielsen: *Modelling of Deteriorating RC-Structures under Stochastic Dynamic Loading by Neural Networks.* ISSN 0902-7513 R9409.

PAPER NO. 126: H. U. Köylüoğlu, S. R. K. Nielsen & A. Ş. Çakmak: *Reliability Approximations for MDOF Structures with Random Properties subject to Random Dynamic Excitation in Modal Subspaces.* ISSN 0902-7513 R9440.

PAPER NO. 127: H. U. Köylüoğlu, S. R. K. Nielsen and A. Ş. Çakmak: *A Faster Simulation Method for the Stochastic Response of Hysteretic Structures subject to Earthquakes.* ISSN 0902-7513 R9523.

PAPER NO. 128: H. U. Köylüoğlu, S. R. K. Nielsen, A. Ş. Çakmak & P. H. Kirkegaard: *Prediction of Global and Localized Damage and Future Reliability for RC Structures subject to Earthquakes.* ISSN 0901-7513 R9426.

PAPER NO. 129: C. Pedersen & P. Thoft-Christensen: *Interactive Structural Optimization with Quasi-Newton Algorithms.* ISSN 0902-7513 R9436.

PAPER NO. 130: I. Enevoldsen & J. D. Sørensen: *Decomposition Techniques and Effective Algorithms in Reliability-Based Optimization.* ISSN 0902-7513 R9412.

PAPER NO. 131: H. U. Köylüoğlu, S. R. K. Nielsen & A. Ş. Çakmak: *Approximate Forward Difference Equations for the Lower Order Non-Stationary Statistics of Geometrically Non-Linear Systems subject to Random Excitation.* ISSN 0902-7513 R9422.

STRUCTURAL RELIABILITY THEORY SERIES

PAPER NO. 132: I. B. Kroon: *Decision Theory applied to Structural Engineering Problems.* Ph.D.-Thesis. ISSN 0902-7513 R9421.

PAPER NO. 134: H. U. Köylüoğlu, S. R. K. Nielsen & A. Ş. Çakmak: *Solution of Random Structural System subject to Non-Stationary Excitation: Transforming the Equation with Random Coefficients to One with Deterministic Coefficients and Random Initial Conditions.* ISSN 0902-7513 R9429.

PAPER NO. 135: S. Engelund, J. D. Sørensen & S. Krenk: *Estimation of the Time to Initiation of Corrosion in Existing Uncracked Concrete Structures.* ISSN 0902-7513 R9438.

PAPER NO. 136: H. U. Köylüoğlu, S. R. K. Nielsen & A. Ş. Çakmak: *Solution Methods for Structures with Random Properties subject to Random Excitation.* ISSN 0902-7513 R9444.

PAPER NO. 137: J. D. Sørensen, M. H. Faber & I. B. Kroon: *Optimal Reliability-Based Planning of Experiments for POD Curves.* ISSN 0902-7513 R9455.

PAPER NO. 138: S.R.K. Nielsen & P.S. Skjærbæk, H.U. Köylüoğlu & A.Ş. Çakmak: *Prediction of Global Damage and Reliability based upon Sequential Identification and Updating of RC Structures subject to Earthquakes.* ISSN 0902-7513 R9505.

PAPER NO. 139: R. Iwankiewicz, S. R. K. Nielsen & P. S. Skjærbæk: *Sensitivity of Reliability Estimates in Partially Damaged RC Structures subject to Earthquakes, using Reduced Hysteretic Models.* ISSN 0902-7513 R9507.

PAPER NO. 142: S. R. K. Nielsen & R. Iwankiewicz: *Response of Non-Linear Systems to Renewal Impulses by Path Integration.* ISSN 0902-7513 R9512.

PAPER NO. 145: H. U. Köylüoğlu, S. R. K. Nielsen, Jamison Abbott and A. Ş. Çakmak: *Local and Modal Damage Indicators for Reinforced Concrete Shear Frames subject to Earthquakes.* ISSN 0902-7513 R9521

PAPER NO. 146: P. H. Kirkegaard, S. R. K. Nielsen, R. C. Micaletti and A. Ş. Çakmak: *Identification of a Maximum Softening Damage Indicator of RC-Structures using Time-Frequency Techniques.* ISSN 0902-7513 R9522.

PAPER NO. 147: R. C. Micaletti, A. Ş. Çakmak, S. R. K. Nielsen & P. H. Kirkegaard: *Construction of Time-Dependent Spectra using Wavelet Analysis for Determination of Global Damage.* ISSN 0902-7513 R9517.

PAPER NO. 149: P. S. Skjærbæk, S. R. K. Nielsen & A. Ş. Çakmak: *Damage Location of Severely Damaged RC-Structures based on Measured Eigenperiods from a Single Response.* ISSN 0902-7513 R9518.

Department of Building Technology and Structural Engineering
Aalborg University, Sohngaardsholmsvej 57, DK 9000 Aalborg
Telephone: +45 98 15 85 22 Telefax: +45 98 14 82 43